10
Light Scattering by Polymer Solutions

Nature, and Nature's Laws lay hid in Night.
God said, *Let Newton be!* and All was Light.

Epitaph for Isaac Newton, Alexander Pope

10.1 Introduction

This chapter is the narrowest in scope of any chapter in this book. In it we discuss a single experimental procedure and its interpretation. It is appropriate to examine light scattering in considerable detail, since the theory underlying this method is relatively unfamiliar to students and the interpretation yields information concerning a variety of polymer parameters.

There are really only two major conclusions presented in the chapter, and even these can be consolidated into a single analysis when applied to experimental data. First, we shall develop the Rayleigh theory for the scattering of light by molecules whose linear dimensions are small compared to the wavelength of the light. For visible light Rayleigh scattering applies to gases and low molecular weight liquids, and we discuss these applications as part of the process for gaining understanding of this powerful technique. Next we derive the Debye theory for scattering by particles whose dimensions are no longer insignificant compared to the wavelength of light. This theory corrects Rayleigh scattering for interference effects and therefore includes the assumptions and limitations of Rayleigh scattering, plus some added features of its own.

Although we take a while before eventually casting these theories in forms which are directly applicable to polymers, the final results are highly practical. Throughout the chapter the presentation is aimed toward these eventual applications. We begin by comparing and contrasting the turbidity of solutions which scatter light with the absorbance of solutions which absorb light. We describe the experiments whereby scattering data are collected, and discuss the extrapolation procedures that must be followed to match experimental results with

theoretical models. Although we develop the various stages stepwise, we conclude by describing the Zimm method for combining all extrapolations in a single graphical method. Through these manipulations of light-scattering data, absolute values of the molecular weight, the second virial coefficient, and the radius of gyration can all be determined. Thus a single procedure can be used to evaluate several different parameters which would otherwise entail more than one kind of experiment. In contrast with osmometry, light scattering is rapid and free from complications associated with finding a suitable membrane. In contrast with viscometry and GPC, light scattering is absolute and does not require prior calibration. In spite of these advantages, light scattering has some limitations of its own which we shall discover as the theory unfolds. Leaving their respective limitations aside, we see that light scattering and osmometry complement each other, since each gives a different kind of molecular weight average; therefore, taken together, they provide information about the width of the molecular weight distribution.

This chapter is the only place in this volume that we encounter electrical units. Certain equations in electrostatics differ by the factor 4π, depending on whether they are written for SI or cgs units. To help clarify this situation, the chapter contains an appendix on electrical units which may be helpful, particularly when references based on other units are consulted.

10.2 The Intensity of Scattered Light and Turbidity

Chemistry students are familiar with spectrophotometry, the qualitative and quantitative uses of which are widespread in contemporary chemistry. The various features of absorption spectra are due to the absorption of radiation to promote a particle from one quantized energy state to another. The scattering phenomena we discuss in this chapter are of totally different origin: classical not quantum physics. However, because of the relatively greater familiarity of absorption spectra, a comparison between absorption and scattering is an appropriate place to begin our discussion.

We begin with a consideration of notation, defining I_0 as the intensity of light incident (subscript 0) upon a sample and I_t as the intensity of the light transmitted (subscript t) through a sample of thickness x. There are two different mechanisms that can account for the fact that $I_t < I_0$:

1. When the energy of the light matches the spacing of quantum states, some light is absorbed. In this case $I_0 - I_t = I_{abs}$.
2. When light interacts with the electrons in molecules in a nonquantized fashion, some of the incident light is redistributed in all directions, that is, scattered. As a result of this redistribution, $I_t < I_0$, with $I_0 - I_t = I_{sca}$.
3. It items (1) and (2), the effects are considered separately, although they may both occur together. When absorption is the primary interest, it is

rarely necessary to consider the accompanying scattering, since the latter contributes far less than absorption to the attenuation of intensity. When scattering is the primary interest, it is generally investigated in a portion of the spectrum which is free from absorption peaks. We shall always assume the latter situation, although scattering theories for absorbing particles are also available.

Figure 10.1 schematically illustrates the relationship between I_0, I_t, and I_s.

In spectrophotometry the absorbance per unit length of path through the sample ϵ is defined as

$$\epsilon = - \ln\left(\frac{I_t}{I_0}\right) \tag{10.1}$$

In the absence of absorption, scattering alone is responsible for any attenuation; therefore

$$\epsilon = - \ln\left(\frac{I_0 - I_s}{I_0}\right) = - \ln\left(1 - \frac{I_s}{I_0}\right) \cong \frac{I_s}{I_0} \tag{10.2}$$

where the last approximation is justified since the scattering intensity is ordinarily quite small. It does not make much sense to call this quantity "absorbance" when no absorption is involved; the scattering equivalent is called turbidity and given the symbol τ. These ideas enable us to write $(I_t/I_0)_{abs} = \exp(-\epsilon x)$,

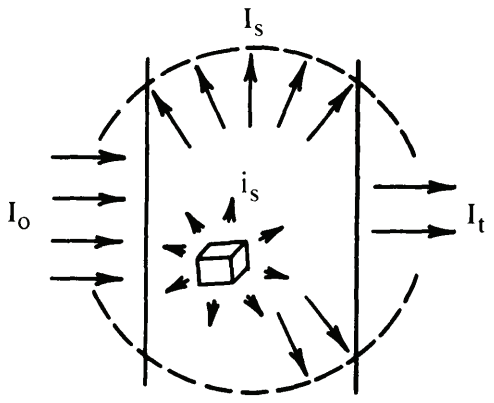

Figure 10.1 Relationships between I_0, I_t, and I_s. The light scattered per unit volume i_s is also shown.

$(I_t/I_0)_{sca} = \exp(-\tau x)$ and $(I_t/I_0)_{net} = \exp[-(\epsilon + \tau)x]$ for the situations itemized above. The turbidity of a specimen, then, is experimentally equivalent to absorption, except it is a small ($\tau \ll \epsilon$), classical effect which is generally ignored in absorption studies. To prevent it from being overshadowed by absorption, we consider nonabsorbing systems for which $\epsilon = 0$.

Like ϵ, τ is the product of two contributions: the concentration N/V of the centers responsible for the effect and the contribution per particle to the attenuation. It may help us to become oriented with the latter to think of the scattering centers as opaque spheres of radius R. These project opaque cross sections of area πR^2 in the light path. The actual cross section is then multiplied by the scattering efficiency factor Q_{sca}, so that $\pi R^2 Q_{sca}$ gives the *optical* cross section of the particle. The fact that the actual particle may not be opaque or spherical is taken into account by Q_{sca}. Thus we can think of the turbidity as the product of three factors:

$$\tau = (\pi R^2)\, Q_{sca} \left(\frac{N}{V}\right) \tag{10.3}$$

At this point it is instructive to examine the units of each of the terms in Eq. (10.3):

1. τ has units of length^{-1}. By analogy with Eq. (10.1), it is the "absorbance" per unit path length.
2. πR^2 has the units of length^2, since it is an area. This is the case regardless of the geometry of the actual particle.
3. N/V has units of length^{-3}, since it is a concentration.

It is apparent from these considerations that Q_{sca} is dimensionless. It is also clear that neither πR^2 nor N/V have anything to do with the wavelength λ of the light used in the experiment. In spite of this, τ is wavelength dependent, showing a broad, smooth variation with λ—as opposed to sharp peaks—for nonabsorbing particles. What this means is that the wavelength dependence of τ enters Eq. (10.3) through Q_{sca}. Furthermore, since Q_{sca} is dimensionless, λ must enter Q_{sca} in the form of a ratio, with some other variable having units of length. A fairly obvious choice for the latter is R, since Q_{sca} is a property of the scattering center.

An important aspect of the realization that Q_{sca} can be represented by $f(R/\lambda)$ is the fact that the function has the same value for any particles with the same R/λ ratio. Thus x rays interacting with atoms and microwaves interacting with fog drops have about the same R/λ ratio as polymer molecules interacting with visible light. As far as the size dependence of Q_{sca} is concerned, all of these systems are described by the same value of Q_{sca}, provided that the wavelength of the illumination is scaled to make the R/λ ratio the same in all cases.

The purpose of these qualitative remarks is to show that turbidity experiments are potential sources of information concerning both the spatial extension ($\propto$ R) of the scatterers and their molecular weight (since $N/V \propto c_2/M$). We anticipated these conclusions earlier in this volume by noting elsewhere that light scattering provides absolute values for the radius of gyration and the weight average molecular weight of a polymer.

In developing these ideas quantitatively, we shall derive expressions for the light scattered by a volume element in the scattering medium. The symbol i_s is used to represent this quantity; its physical significance is also shown in Fig. 10.1. [Our problem with notation in this chapter is too many i's!] Before actually deriving this, let us examine the relationship between i_s and I_s or, more exactly, between i_s/I_0 and I_s/I_0.

In order to do this, we anticipate the form of the expression for i_s/I_0. Equation (10.31) will show that i_s/I_0 can be written as the product of two terms: an optical-molecular factor we symbolize as R_ϕ and a geometrical factor $1 + \cos^2 \phi_x/r^2$, where r is the distance from the scattering molecule and ϕ_x is the angle between the x axis and a specific line of sight. The unscattered—that is, incident and transmitted—light beam in Fig. 10.1 is assumed to travel in the x direction. Accordingly, the total scattered intensity I_s is equal to the summation *over all angles* of the scattering per unit volume, i_s. The factor R_ϕ does not affect this summation and can be factored out. For the present we are only concerned with the summation:

$$\frac{I_s}{I_0} = \sum_{\substack{\text{all} \\ \text{angles}}} \frac{i_s}{I_0} = \int_0^\pi \frac{i_s}{I_0} 2\pi r \sin \phi_x \, (r \, d\phi_x) \tag{10.4}$$

The justification for replacing the summation with this integral is seen by examining Fig. 10.2. An element of area on the surface of a sphere of radius r has a circumference $2\pi r \sin \phi_x$ and a thickness $r \, d\phi_x$. Integration of these increments of area gives the light scattered at all angles. As noted above, $i_s/I_0 = R_\phi (1 + \cos^2 \phi_x)/r^2$. Substituting this into Eq. (10.4) and canceling the r^2's gives

$$\frac{I_s}{I_0} = 2\pi R_\phi \int_0^\pi (1 + \cos^2 \phi_x) \sin \phi_x \, d\phi_x \tag{10.5}$$

This standard integral is readily evaluated to give the numerical factor 8/3; therefore

$$\tau = \frac{I_s}{I_0} = \frac{16\pi}{3} R_\phi \tag{10.6}$$

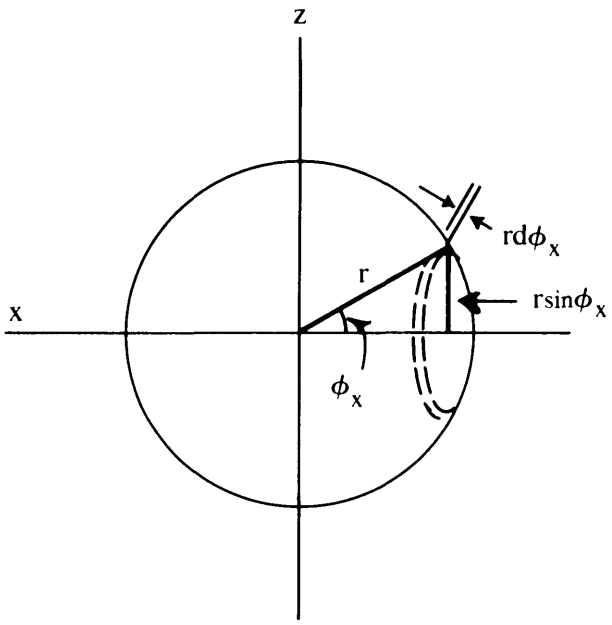

Figure 10.2 Definition of an element of area for the purpose of integrating $i_s(r, \phi_x)$ over all angles to evalute I_s. (Reprinted from Ref. 2, p. 178.)

In Sec. 10.5 we shall consider the derivation of i_s/I_0 and the factor R_ϕ which appears in Eq. (10.6). First, however, it is worthwhile to review some basic ideas about light itself.

10.3 Electric Fields and Their Interaction with Matter

The scattering of visible light by polymer solutions is our primary interest in this chapter. However, since Q_{sca} is a function of the ratio R/λ, as we saw in the last section, the phenomena we discuss are applicable to the entire range of the electromagnetic spectrum. Accordingly, a general review of the properties of this radiation and its interactions with matter is worthwhile before a specific consideration of scattering.

In this discussion we define the x direction to be the direction of propagation of the light waves. This means that the yz plane contains the oscillating electrical and magnetic fields which carry the energy of the radiation. Only the electric field concerns us in scattering. Since the oscillation is periodic in both time t and location x, the electric field can be represented by the equation

$$E = E_0 \cos\left[2\pi\left(\nu t + \frac{x}{\lambda}\right)\right] \tag{10.7}$$

in which the following applies:

1. ν is the frequency and at a fixed location—say, $x = 0$—one full wave is traced out in a time $1/\nu$.
2. λ is the wavelength and at a fixed time—say, $t = 0$—one full wave is traced out over a distance λ.
3. E_0 is the maximum amplitude of the field, since the cosine factor which modifies it oscillates between -1 and $+1$.
4. E oscillates in sign, as described by Eq. (10.7), yet the wave manifests itself with an intensity which is always positive. This suggests that E^2 rather than E itself be used as a measure of light intensity.
5. E causes a particle of charge q to experience a force and hence a displacement. Both the force and the displacement are proportional to E; therefore the energy of the field-charge interaction—the product of the force and the displacement—is proportional to E^2.
6. The combination of items (4) and (5) leads to the important conclusion that light intensity is the measure of the flux of energy through a surface perpendicular to the direction of propagation—the yz plane in our convention—and this is proportional to E^2.

Under vacuum, the velocity of propagation c of an electromagnetic wave is 3.0×10^8 m sec^{-1}, and this is related to the frequency and wavelength by

$$c = \nu\lambda_0 \tag{10.8}$$

In a medium of refractive index $\tilde{n}$, both c and λ_0 are decreased to $1/\tilde{n}$ of their value under vacuum: $v = c/\tilde{n}$ and $\lambda = \lambda_0/\tilde{n}$:

$$v = \nu\lambda \tag{10.9}$$

Note that c and λ_0 are used as symbols for velocity and wavelength, respectively, under vacuum, and that v and λ signify their counterparts in some medium. In addition, we observe that the frequency ν is not affected by the passage from one medium to another. As the light passes through a substance, its electric field interacts with the electrons of that substance, inducing oscillations in them at the same frequency as the frequency of the original field. Since no change in frequency is involved in going from vacuum into matter, it is the wavelength that must also adjust along with velocity. Figure 10.3 illustrates this by showing successive crests of electromagnetic waves traveling in the direction of the arrow as they pass from vacuum into a substance of refractive index $\tilde{n}$. At the surface

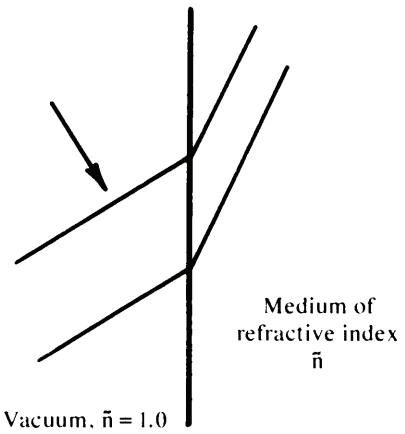

Figure 10.3 Schematic illustration showing the bending of light and the decrease in wavelength as the radiation passes from a vacuum to a medium of refractive index ñ.

between the two media, there is a continuity in E with respect to frequency. That is, from whichever side of the surface it is viewed, the trace of E on the boundary is the same. To achieve this "fit," the wave front bends, as shown in Fig. 10.3, and the spacing between the wave crests, the wavelength, decreases. Both the bending of light and the change in wavelength are required by the continuity of E at the interface.

As our discussion of scattering proceeds, we shall examine the coupling between the oscillating electrical field of light and the electrons of the scatterer in detail. First, it is useful to consider the interaction of an electric field with matter, as this manifests itself in the dielectric behavior of a substance. This will not only introduce us to the field-matter interaction, but will also provide some relationships which will be useful later.

For this purpose we compare a parallel plate capacitor under vacuum and one containing a dielectric, as shown in Figs. 10.4a and b, respectively. The plates of the capacitor carry equal but opposite charges ±Q which can be described as $\pm\sigma A$, where σ is the surface charge density and A is the area of the plates. In this case, the field between the plates is given by

$$E_0 = \frac{\sigma}{\epsilon_0} \tag{10.10}$$

where ϵ_0 is the permittivity of vacuum, 8.85×10^{-12} C^2 J^{-1} m^{-1}. If the space between the plates is filled with a dielectric as shown in Fig. 10.4b, the field is decreased to a value

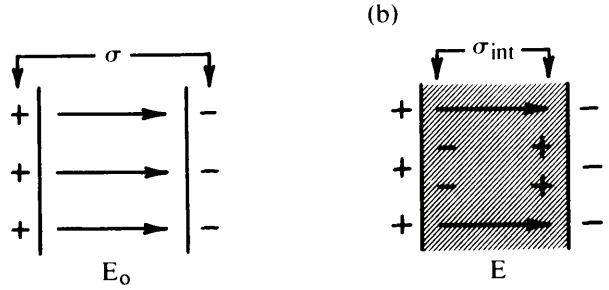

Figure 10.4 Parallel-plate capacitor with surface charge density σ. (a) The field is E_0 with no dielectric present. (b) The field is reduced to E by a dielectric which acquires a surface charge of its own, σ_{int}.

$$E = \frac{\sigma}{\epsilon} \tag{10.11}$$

where the ratio $\epsilon/\epsilon_0 = \epsilon_r$ is called the relative dielectric constant of the medium and is measured as the ratio of the capacitances of the apparatus with and without the substance. Sometimes the term *relative permittivity* and the symbol K_r are used instead of ϵ_r to describe this ratio.

Since $\epsilon > \epsilon_0$, we seek to explain the smaller field in the presence of the dielectric in terms of molecular properties and the way in which they are affected by the electric field. An easy way to visualize the effect is to picture an opposing surface charge—indicated as σ_{int} in Fig. 10.4b—accumulating on the dielectric. This partially offsets the charge on the capacitor plates to a net charge density $\sigma - \sigma_{int}$ so that E_0 becomes E and is given by

$$E = \frac{\sigma - \sigma_{int}}{\epsilon_0} \tag{10.12}$$

Next we can eliminate σ from Eqs. (10.11) and (10.12) to obtain

$$\sigma_{int} = \epsilon_0 (\epsilon_r - 1)E \tag{10.13}$$

Now let us examine the molecular origin of σ_{int}. Molecular polarity may be the result of either a permanent dipole moment μ or an induced dipole moment μ_{ind}, where the latter arises from the distortion of the charge distribution in a molecule due to an electric field. We saw in Chap. 8 that each of these types of polarity are sources of intermolecular attraction. In the present discussion we assume that no permanent dipoles are present and note that the induced dipole moment is proportional to the net field strength at the molecule:

$$\mu_{ind} = \alpha E_{net} \tag{10.14}$$

where α is called the polarizability of the molecule. It is apparent from this definition that the larger α is, the greater is the induced dipole moment per unit field. Thus α is aptly named, since it measures the ability of a molecule to undergo polarization.

Next we consider the net field at the molecule. This turns out to be the sum of two effects: the macroscopic field given by Eq. (10.12) plus a local field that is associated with the charge on the surface of the cavity surrounding the molecule of interest. The latter may be shown to equal $(1/3)(\sigma_{int}/\epsilon_0)$. Hence the net field at the molecule is

$$E_{net} = E + \frac{1}{3}\frac{\sigma_{int}}{\epsilon_0} = \frac{\sigma_{int}}{\epsilon_0(\epsilon_r - 1)} + \frac{1}{3}\frac{\sigma_{int}}{\epsilon_0} = \frac{\sigma_{int}}{3\epsilon_0}\left(\frac{\epsilon_r + 2}{\epsilon_r - 1}\right) \tag{10.15}$$

All that remains to be done is to connect σ_{int} with μ_{ind}. This is done by the observation that $\sigma_{int} = Q_{int}/A$, where Q_{int} is the charge on the surface of the dielectric. Next, Q_{int}/A can be written $(Q_{int}/V)d$, where V and d are the volume and the thickness of the dielectric, respectively. The product of a charge and the distance that separates it from its opposite charge defines a dipole moment. This means that σ_{int} has the significance of a net dipole moment per unit volume for the sample. If only induced dipole moments operate, as we have specified, this net dipole per unit volume is simply the product of the number of molecules per unit volume $\rho N_A/M$ and the induced dipole moment of each: $\sigma_{int} = (\rho N_A/M)\mu_{ind}$. Combining this idea with Eqs. (10.14) and (10.15) gives

$$\sigma_{int} = \frac{\rho N_A \alpha}{M}\left[\frac{\sigma_{int}}{3\epsilon_0}\left(\frac{\epsilon_r + 2}{\epsilon_r - 1}\right)\right] \tag{10.16}$$

or

$$\frac{1}{3}\frac{\rho N_A \alpha}{M\epsilon_0} = \frac{\epsilon_r - 1}{\epsilon_r + 2} \tag{10.17}$$

This result, called the Clausius-Mosotti equation, gives the relationship between the relative dielectric constant of a substance and its polarizability, and thus enables us to express the latter in terms of measurable quantities. The following additional comments will connect these ideas with the electric field associated with electromagnetic radiation:

1. If molecules have permanent dipole moments and can orient themselves with respect to the field, then Eq. (10.17) must be modified by inclusion of a term associated with μ.

2. In discussing capacitance, we implied nothing about the frequency of the field. The results given are general, applying equally to the frequencies of alternating current and of the electric field in electromagnetic radiation.
3. At the high frequencies of visible light, any permanent dipoles present cannot respond rapidly enough to contribute to the dielectric behavior; hence Eq. (10.17) applies to polar molecules also under the influence of light.
4. Under the same conditions, Maxwell's theory of radiation shows that the refractive index and the relative dielectric constant are simply related by

$$\epsilon_r = \tilde{n}^2 \tag{10.18}$$

Both ϵ_r and $\tilde{n}$ are clearly frequency dependent, since the foregoing argument shows that various effects contribute to the polarity of a molecule at different frequencies.

Equations (10.17) and (10.18) show that both the relative dielectric constant and the refractive index of a substance are measurable properties of matter that quantify the interaction between matter and electric fields of whatever origin. The polarizability is the molecular parameter which is pertinent to this interaction. We shall see in the next section that α also plays an important role in the theory of light scattering. The following example illustrates the use of Eq. (10.17) to evaluate α and considers one aspect of the applicability of this quantity to light scattering.

Example 10.1

The refractive index of CCl_4 at 20°C and 589 nm, the D line of the sodium spectrum, is 1.4607. At this temperature the density of this compound is 1.59 g cm^{-3}. Use this information to calculate α for CCl_4. Criticize or defend the following proposition: The prediction that $Q_{sca} = f(R/\lambda)$ may have been premature. The consideration of Eq. (10.3) which led to this conclusion could just as well predict $Q_{sca} = f(\alpha^{1/3}/\lambda)$.

Solution

According to Eq. (10.18), $\epsilon_r = \tilde{n}^2 = (1.4607)^2 = 2.1336$ at $\nu = 5.09 \times 10^{14}$ Hz (589 nm). The number of CCl_4 molecules at 20°C is given by

$$\frac{\rho N_A}{M} = \frac{(1.59 \text{ g cm}^{-3})(6.02 \times 10^{23} \text{ molecules mol}^{-1})}{153.8 \text{ g mol}^{-1}}$$

$$= 6.245 \times 10^{21} \text{ molecules cm}^{-3}$$

Therefore, by Eq. (10.17),

$$\alpha = \frac{3\epsilon_0(\epsilon_r - 1)/(\epsilon_r + 2)}{\rho N_A/M} = \frac{3(8.85 \times 10^{-12}\ \mathrm{J^{-2}\ C^{-2}\ m^{-1}})(0.2742)}{6.245 \times 10^{21}\ \mathrm{molecules\ cm^{-3}}}$$

$$= 1.166 \times 10^{-39}\ \mathrm{C^2\ J^{-1}\ m^2\ molecule^{-1}}$$

This is the correct value for α in SI units, as can be verified by examining the units in Eq. (10.14): αE_{net} has units $(\mathrm{C^2\ J^{-1}\ m^2})(\mathrm{V\ m^{-1}}) = \mathrm{C\ m}$, which is correct for μ_{ind}. In this instance cgs units are also informative; to effect the transformation we divide by $4\pi\epsilon_0$ as described in the appendix, Sec. 10.12:

$$\alpha_{cgs} = \frac{\alpha}{4\pi\epsilon_0} = \frac{1.166 \times 10^{-39}\ \mathrm{C^2\ J^{-1}\ m^2\ molecule^{-1}}}{1.113 \times 10^{-10}\ \mathrm{C^2\ J^{-1}\ m^{-1}}}$$

$$= 1.05 \times 10^{-29}\ \mathrm{m^3\ molecule^{-1}} = 10.5\ \mathrm{\AA^3\ molecule^{-1}}$$

Expressed in these units, α resembles a molecular volume; hence $\alpha^{1/3}$ has units of length and is thus a length which characterizes the interaction between a molecule and the field. In view of this, it may be true that $Q_{sca} = f(\alpha^{1/3}/\lambda)$, since all we can say about Q_{sca} is that it is dimensionless.

•

With this as background, we are finally in a good position to look at the scattering process itself.

10.4 Light Scattering by an Isolated Molecule

Ordinarily, light-scattering experiments are conducted with unpolarized light, but the following discussion is more easily visualized in terms of light which is linearly polarized. For light propagating in the x direction, the electric field lies in the yz plane and may be resolved into y and z components. Polarizing filters have different absorption coefficients in perpendicular directions, and hence absorb light in which the field oscillates in one direction and pass the perpendicular component. For convenience, we speak of vertically and horizontally polarized light when the oscillations are parallel to the z and y axes, respectively.

To quantify the interaction between a molecule and an incident ray of light, we imagine the molecule situated at the origin of a coordinate system as shown in Fig. 10.5 and consider its interaction with vertically polarized light traveling in the x direction. Since it is the mobile charge in the molecule that couples with the light, we represent the molecule as a quantity of charge q. As discussed in the last section, the oscillating field induces an oscillation in the charge q,

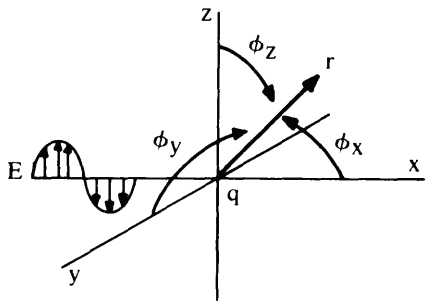

Figure 10.5 Definition of the variables used to describe the electric field produced by the oscillation of the charge q under the influence of vertically polarized light. (Reprinted from Ref. 2, p. 164.)

and it is a basic fact of electromagnetism that this situation is a source of radiation. On a molecular scale this molecule behaves like an antenna, sending out a signal along a line of sight represented by the arrow in Fig. 10.5. The radial distance from the radiating dipole is r and the angles between the line of sight and the coordinate axes are designated ϕ_x, ϕ_y, and ϕ_z, respectively.

Since the charge becomes coupled with the oscillating field, q undergoes a periodic acceleration which we represent by a_p. Next we borrow a relationship from electromagnetic theory to describe the field produced by an oscillating dipole such as the molecule we have described:

$$E = \frac{q a_p \sin \phi_z}{4\pi\epsilon_0 c^2 r} \tag{10.19}$$

Since we have introduced this relationship without proof, it will be helpful to consider its components with respect to their plausibility:

1. It is reasonable that the field produced by the accelerating charge should be proportional to the magnitude of both the charge and the acceleration.
2. The energy that is radiated spreads out over a solid angle and is therefore proportional to r^{-2}. We saw in Sec. 10.2 that this energy is proportional to E^2; hence E varies with r^{-1}.
3. The factor $4\pi\epsilon_0$ arises from the choice of SI units. Since a_p has units time^{-2}, the acceleration is divided by c^2 to convert the units of the denominator to length^2, as required by the definition of the field.
4. The sin ϕ_z factor shows that the field produced by the oscillator is maximum in the xy plane, zero along the z axis, and symmetrical with respect to the z axis. This geometry is consistent with the vertical polarization of the field which is driving the dipole and producing the field described by Eq. (10.19).

Next we look for a substitution for a_p, the acceleration experienced by the charge. A convenient device for doing this originates from considering the oscillating dipole produced by the driving field. Since $\mu = \alpha E$,we can describe the periodic (subscript p) dipole moment of a molecule by

$$\mu_p = \alpha E_0 \cos(2\pi\nu t) \tag{10.20}$$

where we have used Eq. (10.7) with x = 0 to describe the incident field. Since the dipole moment also equals the charge times the distance of charge separation and it is the latter that is periodic, we identify the displaced charge q as αE_0 and $\xi = \cos(2\pi\nu t)$ as the separation. Therefore the acceleration is

$$a_p = \frac{d^2\xi}{dt^2} = -4\pi^2\nu^2 \cos(2\pi\nu t) \tag{10.21}$$

Substituting these results into Eq. (10.19) gives

$$E = \frac{(\alpha E_0)[-4\pi^2\nu^2 \cos(2\pi\nu t)] \sin\phi_z}{4\pi\epsilon_0 c^2 r} \tag{10.22}$$

for the field produced by the oscillating dipole.

As noted previously, the intensity of light is proportional to the square of the field; hence the intensity of the light radiated by the dipole is given by

$$i_v \propto \frac{\pi^2\nu^4\alpha^2 E_0^2 \cos^2(2\pi\nu t) \sin^2\phi_z}{\epsilon_0^2 c^4 r^2} \tag{10.23}$$

while the intensity of the driving radiation incident (subscript 0) on the molecule is given by squaring Eq. (10.7):

$$I_{0,v} \propto E_0^2 \cos^2(2\pi\nu t) \tag{10.24}$$

The subscript v is attached to both of these intensities as a reminder that the foregoing analysis is based on the assumption of vertical polarization for the incident light beam. The ratio of these intensities gives the fraction of light scattered per molecule by vertically polarized light:

$$\frac{i_v}{I_{0,v}} = \frac{\pi^2\nu^4\alpha^2 \sin^2\phi_z}{\epsilon_0^2 c^4 r^2} = \frac{\pi^2\alpha^2 \sin^2\phi_z}{\epsilon_0^2 \lambda_0^4 r^2} \tag{10.25}$$

Since the vertically polarized light postulated in the derivation of Eq. (10.25) involves both the z component of the electric field and the angle ϕ_z, it is

apparent that the corresponding expression for horizontally (subscript h) polarized light—which involves the y component of the field—is identical to Eq. (10.25), except for the $\sin^2 \phi$ term:

$$\frac{i_h}{I_{0,h}} = \frac{\pi^2 \alpha^2 \sin^2 \phi_y}{\epsilon_0^2 \lambda_0^4 r^2} \tag{10.26}$$

Note that this also involves the assumption of isotropic molecules, which have the same polarizability in all directions. Unpolarized light consists of equal amounts of vertical and horizontal polarization, so the fraction of light scattered in the unpolarized (subscript u) case is given by

$$\frac{i_u}{I_{0,u}} = \frac{1/2\,(i_v + i_h)}{I_{0,u}} = \frac{1}{2} \frac{\pi^2 \alpha^2 (\sin^2 \phi_z + \sin^2 \phi_y)}{\epsilon_0^2 \lambda_0^4 r^2} \tag{10.27}$$

It is awkward to use two different angles to describe the intensity of light scattered along a particular line of sight, but this situation is easily remedied by referring back to Fig. 10.5. It is apparent from Fig. 10.5 that $r \cos \phi$ is the projection of r along either the x, y, or z axis, depending on the choice of ϕ. We therefore see that

$$r^2 (\cos^2 \phi_x + \cos^2 \phi_y + \cos^2 \phi_z) = r^2 \tag{10.28}$$

Replacing $\cos^2 \phi_y$ by $1 - \sin^2 \phi_y$ and $\cos^2 \phi_z$ by $1 - \sin^2 \phi_z$ leads to the relationship

$$\sin^2 \phi_y + \sin^2 \phi_z = 1 + \cos^2 \phi_x \tag{10.29}$$

in terms of which Eq. (10.27) becomes

$$\frac{i_u}{I_{0,u}} = \frac{1}{2} \frac{\pi^2 \alpha^2}{\epsilon_0^2 \lambda_0^4 r^2} (1 + \cos^2 \phi_x) \tag{10.30}$$

The $\sin^2 \phi$ terms in Eqs. (10.25) and (10.26) arise from the consideration of polarized light. The light scattered by polarized incident light is also polarized in the same direction, so the term $1 + \cos^2 \phi_x$ in Eq. (10.30) describes the overall polarization of the scattered light. Before we lose sight of the individual contributions to this, it will be helpful to consider this polarization somewhat further. This is done in the following example.

Example 10.2

Describe the angular dependence of the vertically and horizontally polarized light scattered by a molecule and their resultant by considering the intensity as a vector anchored at the origin whose length in various directions is given by the trigonometric terms in Eqs. (10.25), (10.26), and (10.30).

Solution

The intensity of the vertically polarized scattered light is proportional to $\sin^2 \phi_z$ which, in polar coordinates, is described by a figure 8-shaped curve centered at the origin and having maximum values of ± 1 at $\phi_z = 90°$. Because ϕ_z is symmetrical with respect to the z axis, this component of scattered light is described in three dimensions by a doughnut-shaped surface in which the hole has shrunk to a point - centered symmetrically in the xy plane.

The horizontal component is identical except for its orientation in space. In the horizontal case the "doughnut" lies in the xz plane.

Since the intensities are additive, we can make the following statements about their resultant:

1. Along the z axis, $\sin^2 \phi_z$ contributes nothing but $\sin^2 \phi_y = 1$, so the net scattered light is horizontally polarized.
2. Along the y axis, $\sin^2 \phi_y$ contributes nothing but $\sin^2 \phi_z = 1$, so the net scattered light is vertically polarized.
3. Along the x axis, both $\sin^2 \phi_y$ and $\sin^2 \phi_z$ equal unity. The light consists of equal amounts of horizontally and vertically polarized components, that is, it is unpolarized, and has twice the intensity observed in the perpendicular directions.

This situation is summarized by the term $1 + \cos^2 \phi_x$ in Eq. (10.30), which we now consider. The following table lists some values for this factor for various values of ϕ_x:

ϕ_x (°)	0	15	30	45	60	75	90
$1 + \cos^2 \phi_x$	2.00	1.93	1.75	1.50	1.25	1.07	1.00

These are plotted in Fig. 10.6, which shows the net intensity envelope in the xy plane as a solid line and represents the horizontally and vertically polarized contributions to the resultant by the broken lines. Since ϕ_x is symmetrical with respect to the x axis, the three-dimensional scattering pattern is generated by rotating the solid contour around the x axis.

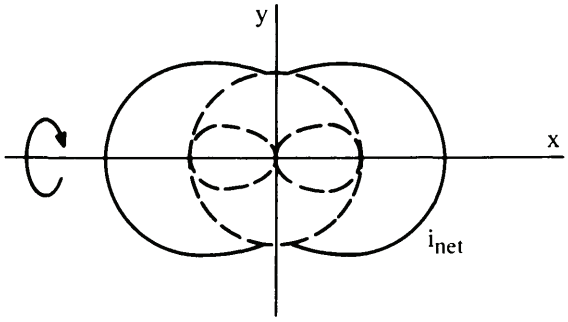

Figure 10.6 Two-dimensional representation of i_v and i_h (broken lines) and their resultant i_{total} (solid line) for scattering by a molecule situated at the origin and illuminated by unpolarized light along the x axis. The intensity in any direction is proportional to the length of the radius vector at that angle. (Reprinted from Ref. 2, p. 168.)

From now on we shall describe the scattered light by Eq. (10.30) exclusively, rather than considering the separate components. We shall also consider ϕ_x only in the xy plane, in which case we use the symbol θ to describe this angle. By convention, the incident light approaches the scattering dipole from $\theta = 180°$, and the transmitted light leaves the sample at $\theta = 0°$.

The equations we have developed in this section describe scattering originating from a point charge located at the origin. Since the charge is, in fact, the electron cloud of a molecule, we must consider the implications of treating a molecule as if it had no spatial extension. The way this consideration explicitly enters the relationships of this section is through the assumption that the dipole "sees" the same field throughout [see Eq. (10.20)]. In visible light, the wavelength is on the order of 500 nm. If the linear dimension of a molecule is small compared to this—as is the case for low molecular weight compounds—then the field is approximately uniform over the dimensions of the molecule and the assumption is valid. For polymer molecules, on the other hand, the dimensions of the molecule may not be insignificant compared to the wavelength of the radiation. In larger particles different parts of the molecule experience significantly different fields, oscillate independently, and produce light which interferes with itself. One way to circumvent this complication appears to be in working with radiation of longer wavelength, but the latter (e.g., infrared) can be absorbed in more ways, so this approach simply trades one source of difficulty for another. It turns out, however, that extrapolating i_s measured at different angles to $\theta = 0°$ also eliminates this interference effect. In Sec. 10.10 we shall discover how the additional complexity of interference can

be interpreted to yield additional information about the scattering source. Before considering this, however, let us further examine the implications of Eq. (10.30) for molecules which are small compared to the wavelength of light.

10.5 Rayleigh Scattering

The scattering formula we have derived in Eq. (10.30) applies to an isolated molecule whose dimensions are small compared to λ. A gas molecule satisfies this description, so we expect that this relationship applies to gases. Since the molecules are far apart in that case, each molecule behaves as an independent scattering center. Therefore the light scattered per unit volume of gas is given simply by the number of molecules per unit volume $\rho N_A/M$ times $i_u/I_{0,u}$. Using the symbol i_s/I_0 for the light scattered per unit volume (unpolarized light is assumed, and the subscript u is dropped), we obtain

$$\frac{i_s}{I_0} = \frac{\rho N_A}{M} \frac{1}{2} \frac{\pi^2 \alpha^2}{\epsilon_0^2 \lambda_0^4} \frac{1 + \cos^2 \theta}{r^2} . \tag{10.31}$$

This is precisely the same quantity we discussed in Sec. 10.2 and illustrated in Fig. 10.1. As anticipated in that section, i_s/I_0 can be written as the product $R_\phi(1 + \cos^2 \theta)/r^2$. In the xy plane, R_ϕ becomes R_θ:

$$R_\theta = \frac{1}{2} \frac{\pi^2 \alpha^2 \rho N_A}{\epsilon_0^2 \lambda_0^4 M} \tag{10.32}$$

which is called the Rayleigh ratio and is given for a gas by Eq. (10.32). By combining Eqs. (10.6) and (10.32), we obtain

$$\tau = \frac{8\pi^3 \alpha^2 \rho N_A}{3M\epsilon_0^2 \lambda_0^4} \tag{10.33}$$

as the turbidity of a gas. Recall from Sec. 10.2 that the turbidity is the analog of absorbance, the light attentuation per unit path through a substance, in the absence of absorption. Equation (10.33) shows that this quantity does the following:

1. It increases with the concentration of scattering centers, which is equivalent to Beer's law.
2. It depends on the nature of the molecules through the factor α^2, where α measures the ability of the molecules to be polarized by an electric field.
3. It varies with the wavelength of the incident radiation as λ_0^{-4}.

The application of this last result to light scattered by the earth's atmosphere is especially interesting. The wavelengths of light at the red and blue ends of the

visible spectrum differ in λ_0 by about a factor of 2, which means that bluish light is scattered about 16 times as much as reddish light. If there were no atmosphere around the earth, the sky would look black, except along direct lines of sight toward the sun or other stars. Instead, we see blue sky overhead where the earth's atmosphere scatters light toward an earthbound observer. This situation is illustrated in Fig. 10.7. Figure 10.7 also shows why sunsets have a reddish hue. In that case the light we see is essentially transmitted light from which the blues have been more effectively removed by scattering. Several additional comments about the color of the sky are pertinent to this discussion:

1. We are explicitly excluding absorption effects: Light-absorbing pollutants modify this description.
2. Skylight is polarized to an extent that depends on the angle between I_0 and I_s in Figs. 10.6 and 10.7.
3. Water drops condensed in the atmosphere have much larger dimensions than gas molecules; hence they are subject to the interference phenomena mentioned at the end of the last section. This alters the color of the scattered light. Smoke and dust particles are also larger and may absorb as well.

The scattering relationships we have considered in this section were published by Lord Rayleigh in 1871 as an explanation for the color and polarization of skylight. Light scattering by small, nonabsorbing particles is known as Rayleigh scattering and is characterized by the λ^{-4} dependence on wavelength. The factor R_θ is known as the Rayleigh ratio of a substance; additional expressions for this quantity in terms of other variables will be developed below.

Before attempting further development of Eq. (10.33), it is useful to examine the dimensions of the various terms in that expression in SI units:

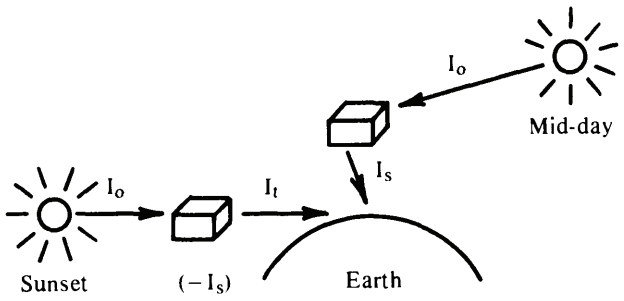

Figure 10.7 Schematic of light reaching an earthbound observer from different regions of the sky.

1. τ is expressed per length of path and has units of meter^{-1}.
2. $\rho N_A/M$ is a concentration and has units of meter^{-3}.
3. λ_0 is the wavelength, so λ_0^{-4} has units of meter^{-4}.
4. The equation is dimensionally consistent if α^2/ϵ_0^2 has units of meter^6. Example 10.2 shows that $\alpha/4\pi\epsilon_0$ has units of meter^3, so the relationship has the proper dimensions.

For the moment, let us define $\alpha/4\pi\epsilon_0$ as α_V, where the subscript V reminds us that the polarizability is being expressed in volume units. Multiplying the numerator and denominator of Eq. (10.33) by $(4\pi)^2$ gives

$$\tau = \frac{128\pi^5}{3} \frac{\alpha_V^2}{\lambda_0^4} \frac{\rho N_A}{M} \tag{10.34}$$

If we think of α_V as a parameter which is proportional to the cube of some kind of molecular "radius" R, then $\alpha_V^2 \propto R^6$ and $\alpha_V^2/\lambda_0^4 \propto R^2(R/\lambda)^4$, which is the form predicted by Eq. (10.3).

The Clausius-Mosotti equation with $\tilde{n}^2$ written for ϵ_r can be used to eliminate α from Eq. (10.33). For gases the refractive index is close to unity, so the factor $\tilde{n}^2 - 1/\tilde{n}^2 + 2$ is approximately

$$\frac{(\tilde{n}+1)(\tilde{n}-1)}{\tilde{n}^2+2} \cong \frac{2}{3}(\tilde{n}-1)$$

Therefore Eq. (10.17) becomes

$$\alpha \cong \frac{2\epsilon_0 M}{\rho N_A}(\tilde{n}-1) \tag{10.35}$$

and Eq. (10.33) is given by

$$\tau = \frac{8\pi^3}{3\lambda_0^4\epsilon_0^2}\left(\frac{2M\epsilon_0}{\rho N_A}(\tilde{n}-1)\right)^2 \frac{\rho N_A}{M} = \frac{32\pi^3}{3\lambda_0^4}(\tilde{n}-1)^2 \frac{M}{\rho N_A} \tag{10.36}$$

An important historic application of this relationship was the determination of Avogadro's number from measurements of light scattered by the atmosphere (see Problem 3).

Next let us consider the light scattered by liquids of low molecular weight compounds. We are actually not directly interested in this quantity per se, but in scattering by solutions–polymer solutions eventually, but for now solutions of small solute molecules. The solvent in such a solution does scatter, but, in practice, the intensity of light scattered by pure solvent is measured and subtracted as a "blank" correction from the scattering by the solution.

Therefore we do not need a theory for scattering by pure liquids to be able to deal with solutions experimentally. The theory for scattering by homogeneous liquids is somewhat simpler to visualize than that for solutions, and the same principles are involved for each. Accordingly, we shall develop the results for pure liquids up to a point and then apply the result to solutions by drawing the appropriate analogy.

The first thing to realize about scattering by liquids is that individual molecules can no longer be viewed as independent scatterers. If a liquid were perfectly uniform in density at the molecular level, its molecules could always be paired in such a way that the light scattered by each member of a pair would be exactly out of phase with the other, resulting in destructive interference. No net scattering results in this case. The second thing to realize, however, is that density is *not* perfectly uniform at the molecular level.

Molecules are in continuous random motion, and as a result of this, small volume elements within the liquid continuously experience compression or rarefaction such that the local density deviates from the macroscopic average value. If we represent by $\delta\rho$ the difference in density between one such domain and the average, then it is apparent that, averaged over all such fluctuations, $\overline{\delta\rho} = 0$: Equal contributions of positive and negative δ's occur. However, if we consider the average value of $\delta\rho^2$, this quantity has a nonzero value. Of these domains of density fluctuation, the following statements can be made:

1. The domain has slightly different properties than its surroundings and can be considered a scattering center itself.
2. Their random, fluctuating nature prevents these domains from destructively interfering with each other's scattered light.
3. The domain is small compared to the wavelength of visible light, so Eq. (10.33) describes the scattering, provided that we can find appropriate values for the concentration and polarizability of these domains.

In the next section we shall pursue the scattering by fluctuations in density. In the case of solutions of small molecules, it is the fluctuations in the solute concentration that plays the equivalent role, so we shall eventually replace $\delta\rho$ by δc_2. First, however, we must describe the polarizability of a density fluctuation and evaluate $\delta\rho$ itself.

10.6 Fluctuations and Rayleigh Scattering

We define the concentration of fluctuation domains at any instant by the symbol N*. In addition, we assume that the polarizability associated with one of these domains differs from the macroscopic average value for the substance

by $\delta\alpha$. As with $\delta\rho$, we expect $\overline{\delta\alpha}$ to equal zero, but $\overline{\delta\alpha^2}$ to have a nonzero value. Accordingly, we can write an expression which is equivalent to Eq. (10.33) for the fluctuations:

$$\tau = \frac{8\pi^3}{3\epsilon_0{}^2\lambda^4}\,\overline{\delta\alpha^2}\,N^* \tag{10.37}$$

Note that the wavelength in vacuum has been replaced by the wavelength in the medium, since it is the latter that drives the oscillations in the fluctuation domain. Now what can we say about $\overline{\delta\alpha^2}$?

The Clausius-Mosotti equation relates the polarizability of a substance to

$$\frac{\epsilon_r - 1}{\epsilon_r + 2} = \frac{\epsilon - \epsilon_0}{\epsilon + 2\epsilon_0}$$

where ϵ is the permittivity of the substance and ϵ_0 is the permittivity of the vacuum that surrounds it. Applied to a fluctuation, we replace ϵ by $\epsilon + \delta\epsilon$ and use ϵ itself rather than ϵ_0 to describe the surroundings. Therefore $(\epsilon - \epsilon_0)/(\epsilon + 2\epsilon_0)$ becomes $\delta\epsilon/(3\epsilon + \delta\epsilon)$, and if we assume that $\delta\epsilon$ is small compared to 3ϵ, Eq. (10.17) becomes

$$\delta\alpha = \frac{\epsilon_0}{N^*}\,\frac{\delta\epsilon}{\epsilon} \tag{10.38}$$

In addition, we can treat the δ's as differential quantities and write

$$\delta\epsilon = \frac{d\epsilon}{d\rho}\,\delta\rho \tag{10.39}$$

Since $\epsilon = \epsilon_r\epsilon_0$ and $\epsilon_r = \tilde{n}^2$ for optical frequencies, Eq. (10.39) becomes

$$\delta\epsilon = \epsilon_0 2\tilde{n}\,\frac{d\tilde{n}}{d\rho}\,\delta\rho \tag{10.40}$$

Combining Eqs. (10.38) and (10.40) gives

$$\overline{\delta\alpha^2} = \frac{\epsilon_0{}^2}{N^{*2}}\left(\frac{\epsilon_0 2\tilde{n}\,d\tilde{n}/d\rho}{\epsilon}\right)^2 \overline{\delta\rho^2} \tag{10.41}$$

where the method of averaging is based on the considerations presented above. Recognizing that $\lambda^{-4}(\epsilon_0/\epsilon)^2 = \lambda^{-4}\,n^{-4} = \lambda_0{}^{-4}$, Eq. (10.41) can be substituted into Eq. (10.37) to yield

$$\tau = \frac{8\pi^3}{3\lambda_0^4} \frac{1}{N^*} \left(2\bar{n} \frac{d\bar{n}}{d\rho}\right)^2 \overline{\delta\rho^2} \tag{10.42}$$

Next we consider how to evaluate the factor $\overline{\delta\rho^2}$. We recognize that there is a local variation in the Gibbs free energy associated with a fluctuation in density, and examine how this value of G can be related to the value at equilibrium, G_0. We shall use the subscript 0 to indicate the equilibrium value of free energy and other thermodynamic quantities. For small deviations from the equilibrium value, G can be expanded about G_0 in terms of a Taylor series:

$$G = G_0 + \left(\frac{\partial G}{\partial \rho}\right)_0 \delta\rho + \frac{1}{2!} \left(\frac{\partial^2 G}{\partial \rho^2}\right)_0 \delta\rho^2 + \cdots \tag{10.43}$$

The quantity $G - G_0 = \delta G$ is the change in G associated with the fluctuation, and the term $(\partial G/\partial\rho)_0\ \delta\rho = 0$ because of the cancellation of positive and negative density fluctuations. Therefore we obtain

$$\delta G \cong \frac{1}{2} \left(\frac{\partial^2 G}{\partial \rho^2}\right)_0 \delta\rho^2 \tag{10.44}$$

Now we evaluate the probability of a fluctuation $\delta\rho$ in terms of a Boltzmann factor:

$$P(\delta\rho) = A \exp\left(-\frac{\delta G}{kT}\right) \tag{10.45}$$

where normalization requires that the constant A be given by

$$\left[\int \exp\left(-\frac{\delta G}{kT}\right) d\,\delta\rho\right]^{-1}$$

integrated over all fluctuations, that is, from $\delta\rho = 0$ to ∞. Using the definition of an average provided by Eq. (1.9), we write

$$\begin{aligned} \overline{\delta\rho^2} &= \frac{\int_0^\infty \delta\rho^2\, e^{-\delta G/kT}\, d\,\delta\rho}{\int_0^\infty e^{-\delta G/kT}\, d\delta\rho} \\ &= \frac{\int_0^\infty \delta\rho^2 \exp\left[-(1/2)(\partial^2 G/\partial\rho^2)_0\, \delta\rho^2/kT\right] d\delta\rho}{\int_0^\infty \exp\left[-(1/2)(\partial^2 G/\partial\rho^2)_0\, \delta\rho^2/kT\right] d\delta\rho} \end{aligned} \tag{10.46}$$

By letting $y = \delta\rho$ and $a = (\partial^2 G/\partial\rho^2)_0/2kT$, these rather formidable-looking integrals are recognized as gamma functions: $\int y^m e^{-ay^2}\, dy$. Using tabulated values for these integrals for $m = 0$ and $m = 2$, we obtain

$$\overline{\delta\rho^2} = \frac{kT}{(\partial^2 G/\partial\rho^2)_0} \tag{10.47}$$

Substitution of this result into Eq. (10.42) yields

$$\tau = \frac{32\pi^3}{3\lambda_0^4}\,\frac{1}{N^*}\left(\tilde{n}\,\frac{d\tilde{n}}{d\rho}\right)^2 \frac{kT}{(\partial^2 G/\partial\rho^2)_0} \tag{10.48}$$

As it stands, Eq. (10.48) is not an encouraging-looking result, but it is actually very close to a highly useful form.

Rather than continuing to discuss the scattering of pure liquids at the theoretical level, let us consider an example to illustrate the application of these ideas.

Example 10.3

By an assortment of thermodynamic manipulations, the quantities $d\tilde{n}/d\rho$ and $[N^*(\partial^2 G/\partial\rho^2)_0]^{-1}$ can be eliminated from Eq. (10.48) and replaced by the measurable quantities α, β, and $d\tilde{n}/dT$: the coefficients of thermal expansion, isothermal compressibility, and the temperature coefficient of refractive index, respectively. With these substitutions, Eq. (10.48) becomes

$$\tau = \frac{32\pi^3}{3\lambda_0^4}\,\frac{kT\beta}{\alpha^2}\,\tilde{n}\,\frac{d\tilde{n}}{dT}^2$$

For benzene†, $\alpha = 1.21 \times 10^{-3}\ \text{deg}^{-1}$, $\beta = 9.5 \times 10^{-10}\ \text{m}^2\ \text{N}^{-1}$, and $d\tilde{n}/dT = 6.38 \times 10^{-4}\ \text{deg}^{-1}$. At 23°C, $\tilde{n} = 1.503$ for benzene at $\lambda_0 = 546$ nm. Use these data to evaluate τ for benzene under these conditions.

Solution

Direct substitution into the equation given provides the required value for τ:

$$\tau = \frac{32\pi^3(1.38 \times 10^{-23}\ \text{J K}^{-1})(296\ \text{K})(9.5 \times 10^{-10}\ \text{m}^2\ \text{N}^{-1})}{3(546 \times 10^{-9}\ \text{m})^4(1.21 \times 10^{-3}\ \text{deg}^{-1})^2(1.503)^2(6.38 \times 10^{-4}\ \text{deg}^{-1})^2}$$

$$= 9.07 \times 10^{-3}\ \text{m}^{-1} \qquad (\text{since J} = \text{N m})$$

●

† M. Kerker, *The Scattering of Light and Other Electromagnetic Radition*, Academic, New York, 1969.

Experimentally the Rayleigh ratio for benzene at 90° has been observed to equal about 1.58×10^{-3} m^{-1} under the conditions described in this example. By Eq. (10.6), $\tau = (16\pi/3)\, R_\theta$ so the value of R_θ corresponding to this calculated turbidity is $R_{\theta,calc} = 5.41 \times 10^{-4}$ m^{-1}. The ratio between the observed value of R_θ and that calculated in the example is called the Cabannes factor and equals about 2.9 in this case.

The origin of this enhanced scattering is understood to originate from the anisotropy of the scattering centers. In terms of the analysis we have presented, this amounts to some scrambling of horizontally and vertically polarized components of light. This means that the light scattered at 90° is not totally polarized as suggested by Fig. 10.6. By using polarizing filters with the detection system, the intensities of the horizontally and vertically polarized components of the scattered light can be measured. The ratio of $i_{s,h}(\theta)$ to $i_{s,v}(\theta)$ is called the depolarization ratio and is given the symbol $\rho_u(\theta)$ (u unpolarized incident light; θ, angle at which measured). The Cabannes factor which corrects for this effect can be evaluated from the measured depolarization ratio. Applied to turbidity, the Cabannes factor C as a function of $\rho_u(90)$ is $C_\tau = [6 + 3\rho_u(90)]/[6 - 7\rho_u(90)]$ and applied to the Rayleigh ratio at 90°, $C_{R_{90}} = [6 + 6\rho_u(90)]/[6 - 7\rho_u(90)]$. Note that for the isotropic scatterers we have assumed, $\rho_u(90) = 0$, so the Cabannes factor equals unity. Corrections of this sort are also required for scattering by solutions. When the turbidity value calculated in Example 10.3 is multiplied by the appropriate Cabannes factor, the calculated and experimental results agree very well. We shall not pursue this correction any further, but shall continue to assume isotropic scatterers; additional details concerning the measurement and use of the Cabannes factor will be found in Ref. 3.

As noted at the end of the last section, it is fluctuations in concentration δc_2 rather than density which act as the scattering centers of interest for solutions of small molecules. There is nothing in the forgoing theory that prevents us from placing $\delta\rho$ by δc_2, the solute concentration in mass volume^{-1} units. Therefore we write for a solution of small molecules

$$\tau = \frac{32\pi^3}{3\lambda_0^4} \frac{1}{N^*} \left(\tilde{n} \frac{d\tilde{n}}{dc_2} \right)^2 \frac{kT}{(\partial^2 G/\partial c_2^2)_0} \tag{10.49}$$

In the next section, we consider the application of Eq. (10.49) to scattering from fluctuations in concentration.

10.7 Light Scattering by Solutions

We saw in Example 10.3 that Eq. (10.48) for the turbidity of pure liquids could be converted to a usable expression by suitable thermodynamic manipulations. The corresponding relationship for solutions can also be transformed into the following useful form:

$$\tau = \frac{32\pi^3}{3\lambda_0^4}\, kT \left(\tilde{n}\,\frac{d\tilde{n}}{dc_2}\right)^2 \frac{c_2}{(\partial\Pi/\partial c_2)_0} \tag{10.50}$$

where $(\partial\Pi/\partial c_2)_0$ describes the concentration dependence of the equilibrium (subscript 0) osmotic pressure. The following outline summarizes the steps involved in this transformation:

1. From the definition of the partial molar quantities [Eq. (8.8)] we write $\delta G = \mu_1 \delta n_1 + \mu_2 \delta n_2$ and $\delta V = \bar{V}_1 \delta n_1 + \bar{V}_2 \delta n_2$, where the δ's refer to an individual fluctuation. The changes in concentration in a fluctuation arise from changes in the number of moles of solvent (subscript 1) and solute (subscript 2), not because of volume changes. Hence $\delta V = 0$; therefore $\delta n_1 = -(\bar{V}_2/\bar{V}_1)\,\delta n_2$ and $\delta G = [\mu_2 - (\bar{V}_2/\bar{V}_1)\,\mu_1]\,\delta n_2$.
2. Since c_2 is expressed as mass volume^{-1}, N* can be related to the δc_2 by the relationship $\delta c_2/M = N^*\delta n_2$. Therefore $\delta G = [\mu_2 - (\bar{V}_2/\bar{V}_1)\,\mu_1]\,(\delta c_2/MN^*)$ or $\partial G/\partial c_2 = [\mu_2 - (\bar{V}_1/\bar{V}_2)\,\mu_1]/MN^*$.
3. Differentiating item (2) again with respect to c_2 gives

$$\frac{\partial^2 G}{\partial c_2^2} = \left(\frac{d\mu_2}{dc_2} - \frac{\bar{V}_2}{\bar{V}_1}\frac{d\mu_1}{dc_2}\right)\Big/ MN^*$$

The Gibbs-Duhem equation also follows from the definition of partial molar quantities: $n_1 d\mu_1 + n_2 d\mu_2 = 0$. With the Gibbs-Duhem equation, $\partial^2 G/\partial c_2^2$ becomes

$$-\left(\frac{n_1}{n_2} + \frac{\bar{V}_2}{\bar{V}_1}\right)\frac{(\partial\mu_1/\partial c_2)_0}{MN^*}$$

4. The factor $[N^*(\partial^2 G/\partial c_2^2)_0]^{-1}$ in Eq. (10.49) can therefore be written

$$\left[-\left(\frac{n_1}{n_2} + \frac{\bar{V}_2}{\bar{V}_1}\right)\frac{(\partial\mu_1/\partial c_2)_0}{M}\right]^{-1} \quad \text{or} \quad \left(-\frac{n_1\bar{V}_1 + n_2\bar{V}_2}{n_2 M}\,\frac{(\partial\mu_1/\partial c_2)_0}{\bar{V}_1}\right)^{-1}$$

Since $c_2 = n_2 M/(n_1\bar{V}_1 + n_2\bar{V}_2)$, this is more concisely written as

$$\left(-\frac{1}{c_2}\,\frac{(\partial\mu_1/\partial c_2)_0}{\bar{V}_1}\right)^{-1}$$

5. Equation (8.79) gives $\mu_1 = \mu_1^0 - \Pi\bar{V}_1$ at equilibrium, so $(\partial\mu_1/\partial c_2)_0 = -\bar{V}_1(\partial\Pi/\partial c_2)_0$, and the factor in item (4) becomes

$$\left[\frac{1}{c_2}\left(\frac{\partial\Pi}{\partial c_2}\right)_0\right]^{-1}$$

Substituting this result into Eq. (10.49) gives Eq. (10.50).

Although Eq. (10.50) is still plagued by remnants of the Taylor series expansion about the equilibrium point in the form of the factor $(\partial\Pi/\partial c_2)_0$, we are now in a position to evaluate the latter quantity explicitly. Equation (8.87) gives an expression for the equilibrium osmotic pressure as a function of concentration: $\Pi = RT(c_2/M + Bc_2^2 + \cdots)$. Therefore

$$\left(\frac{\partial\Pi}{\partial c_2}\right)_0 = RT\left(\frac{1}{M} + 2Bc_2 + \cdots\right) \tag{10.51}$$

in terms of which Eq. (10.50) becomes

$$\tau = \frac{32\pi^3}{3\lambda_0^4 N_A} \frac{(\tilde{n}\, d\tilde{n}/dc_2)^2\, c_2}{(1/M + 2Bc_2)} \tag{10.52}$$

This is the result toward which we have been working. Representing the following cluster of constants by the symbol H, we have

$$H = \frac{32\pi^3 (\tilde{n}\, d\tilde{n}/dc_2)^2}{3\lambda_0^4 N_A} \tag{10.53}$$

Eq. (10.52) can be written

$$\frac{Hc_2}{\tau} = \frac{1}{M} + 2Bc_2 \tag{10.54}$$

This is the equation of a straight line and indicates that a plot of Hc_2/τ versus c_2 has the following properties:

$$\text{slope} = 2B \tag{10.55}$$

and

$$\text{intercept} = \frac{1}{M} \tag{10.56}$$

Thus we have finally established how light scattering can be used to measure the molecular weight of a solute. The concentration dependence of τ enters Eq. (10.54) through an expression for osmotic pressure, and this surprising connection deserves some additional comments:

1. In Chap. 8 we saw how the equilibrium osmotic pressure of a solution is related to ΔG for the mixing process whereby the solution is formed. Any difference in the concentration of the solution involves a change in ΔG_{mix}

and would be reflected by a change in Π. Since the occurrence of a fluctuation in concentration depends on the value of the associated δG, the fluctuation can also be expressed in terms of an equivalent $\delta\Pi$.

2. The value of B given by Eq. (10.55) has exactly the same significance that we discussed for the second virial coefficient in Chap. 8.
3. The limiting value of Hc_2/τ is proportional to $1/M$, which shows that τ/c_2 increases with increasing M, at least if interference effects are ignored. This is just the opposite of the molecular weight dependence of the colligative properties and makes light-scattering experiments ideally suited for polymeric solutes. We shall discuss in Sec. 10.10 the implications of interference effects for solute particles whose dimensions are comparable to λ.
4. For polydisperse systems the molecular weight obtained from light scattering is a weight average value, rather than the number average value obtained from an osmotic pressure experiment. This is an unexpected result in view of the role of Eq. (10.51) in relating τ to M.

It is easy to show that a light-scattering experiment "sees" a polydisperse system in such a way as to average the different molecular weights in terms of their mass rather than their number. We only need to consider the leading term of Eq. (10.54) to see the origin of this effect. For a polydisperse system we write $Hc_{ex}/\tau_{ex} = 1/M$, with $c_{ex} = \Sigma c_i$ and $\tau_{ex} = \Sigma\tau_i$, where the summations extend over all molecular weight categories. For any one molecular weight category it is also true that $Hc_i/\tau_i = 1/M_i$. Combining these various results gives

$$\bar{M} = \frac{\tau_{ex}}{Hc_{ex}} = \frac{\Sigma\tau_i}{H\Sigma c_i} = \frac{H\Sigma c_i M_i}{H\Sigma c_i} = \frac{\Sigma m_i M_i}{\Sigma m_i} \tag{10.57}$$

which is the weight average as defined by Eq. (1.12).

Since the development of a method for polymer characterization has been spread over several sections and since the literature contains several variations in the manner data is displayed, a summary of some pertinent definitions and relationships will be helpful at this point:

1. The relative intensity of light scattered per unit volume i_s/I_0 is a function of factors of three different origins: geometrical (r and θ), optical (λ, $\tilde{n}$, and $d\tilde{n}/dc_2$), and thermodynamic (c_2, M, and B).
2. The Rayleigh ratio combines the intensity factors with those associated with the geometry of the experiment:

$$R_\theta = \frac{i_s}{I_0}\frac{r^2}{1+\cos^2\theta} \tag{10.58}$$

Thus R_θ is a constant in any particular experiment where Rayleigh scattering is obtained, since the entire angular dependence of the light intensity is correctly contained in the $1 + \cos^2 \theta$ term.

3. As the attenuation of the incident beam per unit path through the solution, the turbidity is larger than the Rayleigh ratio by the factor $16\pi/3$, since τ is obtained by integrating R_θ over a spherical surface. Thus, if Eq. (10.54) is written in terms of R_θ rather than τ, the proportionality constant H must also be decreased by $16\pi/3$, in which case the constant is represented by the symbol K:

$$K = \frac{2\pi^2 (\tilde{n}\, d\tilde{n}/dc_2)^2}{\lambda_0^4 N_A} \tag{10.59}$$

and

$$\frac{Kc_2}{R_\theta} = \frac{1}{M} + 2Bc_2 \tag{10.60}$$

4. If turbidity itself is the quantity which is used to characterize a polymer solution, then Eqs. (10.53) and (10.54) are used as derived above:

$$H = \frac{32\pi^3 (\tilde{n}\, d\tilde{n}/dc_2)^2}{3\lambda_0^4 N_A} \tag{10.53}$$

and

$$\frac{Hc_2}{\tau} = \frac{1}{M} + 2Bc_2 \tag{10.54}$$

Figure 10.8 shows two sets of data plotted according to these conventions, after correction for the effect of interference. In Fig. 10.8a, Hc_2/τ is plotted against c_2 for three different fractions of polystyrene in methyl ethyl ketone. Figure 10.8b shows Kc_2/R_θ versus c_2 for solutions of polystyrene in cyclohexane at five different temperatures. These results are discussed further in the following example.

Example 10.4

In both parts of Fig. 10.8, c_2 is expressed in grams per cubic centimeter, with H (or K) and τ (or R_θ) in cgs units also. Verify that the units of the intercept are appropriate units for M^{-1}. Evaluate $\bar{M}_w$ and B for the data in Fig. 10.8a, and $\bar{M}_w$ and Θ from the data in Fig. 10.8b. (K is independent of temperature over the range of T's studied in Fig. 10.8b.)

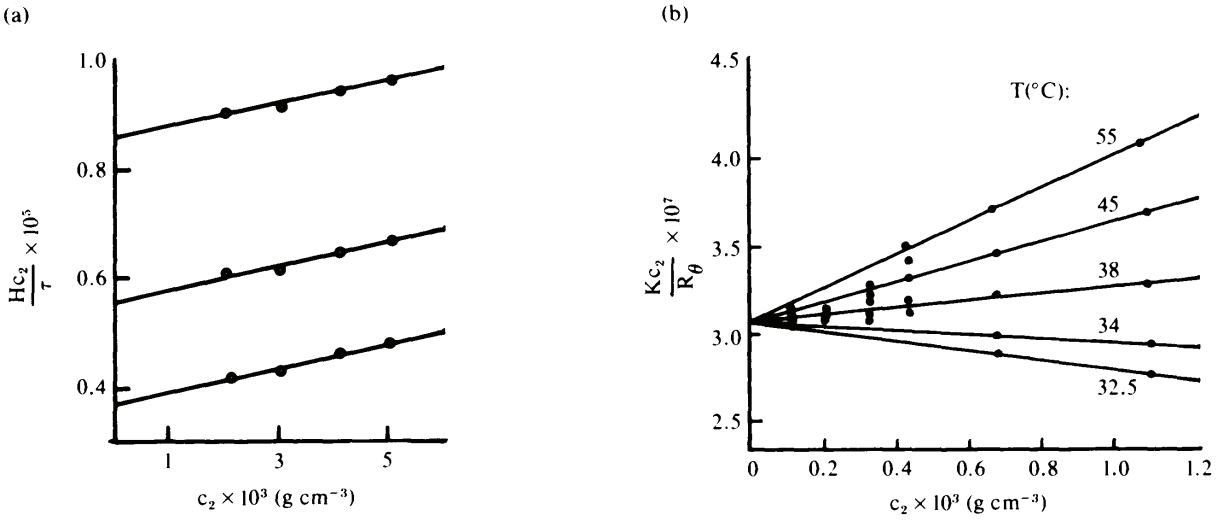

Figure 10.8 Light-scattering data plotted to give slope–intercept values which can be interpreted in terms of M and B. (a) Polystyrene in methyl ethyl ketone. [From B. A. Brice, M. Halwer, and R. Speiser, *J. Opt. Soc. Am.* 40:768 (1950), used with permission.] (b) Polystyrene in cyclohexane at temperatures indicated. Units of ordinates are given in Example 10.4. [Reprinted with permission from W. R. Krigbaum and D. K. Carpenter, *J. Phys. Chem.* 59:1166 (1955), copyright 1955 by the American Chemical Society.]

Solution

Since c_2 has units of grams per cubic centimeter, $\bar{n}\, d\bar{n}/dc_2$ has units of cubic centimeters per gram, because $\bar{n}$ is dimensionless. This means that H (and K) has the cgs units centimeter^2 mole gram^{-2}. τ (and R_θ) has units of centimeter^{-1}, hence Hc_2/τ (and Kc_2/R_θ) has the units moles per gram, which are appropriate for the interpretation of this quantity given by Eq. (10.56). The three lines in Fig. 10.8a have the following intercepts, and the corresponding molecular weights are simply the reciprocals of these values:

$(Hc_2/\tau)_{c=0} \times 10^5$ (mol g^{-1})	0.862	0.556	0.370
$\bar{M}_w$ (g mol^{-1})	116,000	180,000	270,000

Each fraction in Fig. 10.8a has the same slope, and therefore the same value of B is expected. The slope of the lines is approximately $(13 \times 10^{-7}$ mol g$^{-1})/(6 \times 10^{-3}$ g cm$^{-3}) = 2.2 \times 10^{-4}$ cm^3 g^{-2} mol and B = 1.1×10^{-4} cm^3 g^{-2} mol. These are also the correct cgs units for B, as seen by comparison with, say, Eq. (8.97). In Fig. 10.8b the lines for the different temperatures meet at a common intercept of about 3.1×10^{-7} mol g^{-1}, which means that $\bar{M}_w = 3.2 \times 10^6$ g mol^{-1} for the polystyrene sample under investigation. The slopes and B values for the various temperatures are tabulated below:

T (°C)	55	45	38	34	32.5
T (K)	328.2	318.2	311.2	307.2	305.7
Slope $\times 10^5$ (cm^3 g^{-2} mol)	10.76	6.24	2.26	-1.68	-3.06
B $\times 10^5$ (cm^3 g^{-2} mol)	5.38	3.12	1.13	-0.84	-1.53

The Θ temperature is that value of T for which B = 0; therefore Θ can be determined from the results above by graphical interpolation. Although there is some scatter in such a graph, the best value for the temperature at which B = 0 appears to be 308.4 K, which agrees well with values determined for this system by other methods.

Figure 10.8 and Example 10.4 show that light-scattering experiments can be interpreted to yield much the same information as obtained from an osmotic pressure experiment. The fact that the latter yields $\bar{M}_n$ while light scattering gives $\bar{M}_w$ prevents the two methods from being redundant, however. When we discuss interference phenomena in Sec. 10.10, we shall see that the radius of gyration can also be obtained from scattering experiments. Now that the utility of light-scattering experiments in polymer chemistry is well established, let us consider the experimental aspects of this topic.

10.8 Experimental Aspects of Light Scattering

We initiated our discussion of light scattering at the beginning of this chapter by comparing turbidity with the (more familiar) absorbance of a solution. The comparison of these two quantities is also a useful place to begin a consideration of the experimental aspects of light scattering. The components of a spectrophotometer and a light-scattering photometer are largely identical, the primary difference being that absorbance is always measured at $\theta = 0°$, while it is advantageous to measure scattering at various different angles. There are several reasons for using the Rayleigh ratio evaluated at various angles in reporting scattering results:

1. Since i_s is a small quantity, it is better to measure it directly and report it as R_θ rather than by difference, as in the case when turbidity is reported.
2. If experimental values of R_θ are observed to be independent of θ, then Rayleigh scattering is established and Eq. (10.60) can be applied to the data with confidence.
3. If the experimental values of R_θ vary with θ, then the effects of interference are demonstrated. We shall see later in this section that these effects can be eliminated by extrapolating R_θ values to $\theta = 0°$, at which limit Eq. (10.60) also applies.
4. We shall see in subsequent sections that measuring R_θ as a function of θ can be used to evaluate the radius of gyration of the scattering molecules, thereby providing more information about the polymer in addition to M and B.

As a result of these considerations, the primary difference between a spectrophotometer and a light-scattering photometer is the fact that the photodetector is mounted on an arm which pivots at the sample so that intensity measurements can be made at various angles.

Figure 10.9a is a schematic top view of such a photometer, and Fig. 10.9b is a cutaway view of a commercially available instrument which operates on the principles we describe here. The apparatus shown is the Brice-Phoenix universal scattering photometer. Like spectrophotometers, these light-scattering photometers consist of a light source, a sample cell, and a detector, as well as filtering and collimating systems for both the incident and scattered light. The interior of the photometer is painted black and the transmitted beam is absorbed in a light trap to prevent stray light from reaching the detector.

In contrast to spectrophotometry, light-scattering experiments are generally conducted at constant wavelength. Mercury vapor lamps are the most widely used light sources, since the strong lines at 436 and 546 nm are readily isolated by filters to allow monochromatic illumination. Polarizing filters are also included for both the incident and scattered beams so that depolarization can

(a)

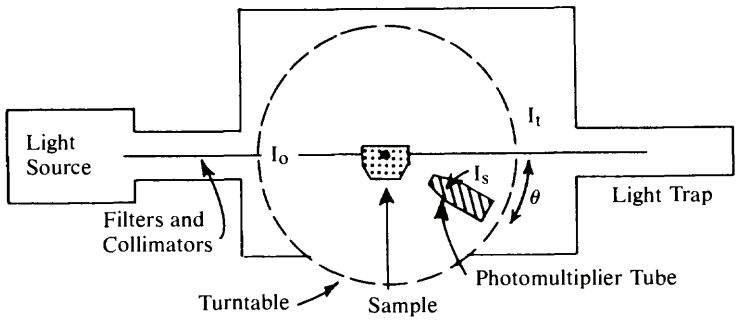

(b)

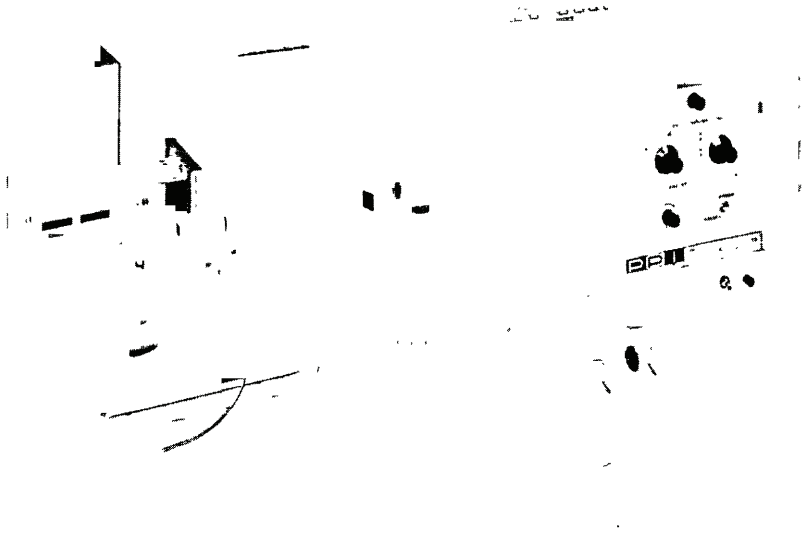

Figure 10.9 Light-scattering photometers. (a) Schematic top view showing movable photodetector. (Reprinted from Ref. 2, p. 176.) (b) Cutaway photograph of commercial light-scattering instrument, the Brice-Phoenix Universal Scattering Photometer. (Photo courtesy of the Virtis Co., Gardiner, New York.)

be studied. The usual assortment of lenses and slits assures that the beams are properly collimated, but these details need not concern us here.

The scattering of laser light is also of considerable importance in contemporary light-scattering practice. As a source of high-intensity monochromatic light, the laser source makes it possible to carry out light-scattering experiments on samples of greatly reduced volume. This means that laser light scattering can be used as a detection system in GPC and also aids in minimizing the scatter produced by dust particles, gas bubbles, and so on, which can invalidate measurements made on larger volumes of solution. Incidentally, as a detection system in GPC, light scattering offers sensitivity to both concentration changes and differences in molecular weight. Combined with refractive index measurements—to supply values for $d\tilde{n}/dc_2$—laser light-scattering detectors provide data which allow for calibration with respect to molecular weight, as well as measure the relative concentrations of the various components.

A variety of cell designs have been successfully employed in light-scattering experiments. Cylindrical cells offer symmetry with respect to viewing angle, but care must be exercised in their use because of reflection from cell walls. This difficulty is not encountered when intensity measurements are made normal to planar cell windows. Cells of octagonal cross section have planar viewing surfaces at $\theta = 0$, 45, 90, 135, and 180°; these are especially convenient for light-scattering experiments.

The solutions must be carefully prepared so as to be free of dust particles and other extraneous scatterers. Filtration through sintered glass or centrifugation is widely used to clarify solutions of particles which would compete with polymeric solutes. This concern for cleanliness also extends to glassware, especially scattering cells. A fingerprint on the viewing window is disastrous!

Photomultipliers are used to measure the intensity of the scattered light. The output is compared to that of a second photocell located in the light trap which measures the intensity of the incident beam. In this way the ratio i_s/I_0 is measured directly with built-in compensation for any variations in the source. When filters are used for measuring depolarization, their effect on the sensitivity of the photomultiplier and its output must also be considered. Instrument calibration can be accomplished using well-characterized polymer solutions, dispersions of colloidal silica, or opalescent glass as standards.

The Rayleigh ratio is not the only optical measurement that must be made in order to interpret light-scattering experiments. In addition, the factor $\tilde{n}\, d\tilde{n}/dc_2$ must also be accurately measured. The refractive index itself is easily determined at the temperature and wavelength of the experiment and requires no further comment. The refractive index gradient $d\tilde{n}/dc_2$, by contrast, presents more of a challenge. Although nominally the slope of a plot of the solution refractive index versus c_2, the gradient is not determined in this manner, since acceptable precision could not be achieved by differences: The solutions

involved are too dilute and the solvent and solute are often not too different in their respective refractive indices.

Instead, the difference between the refractive index of the solvent and that of a solution can be measured directly by one of several designs of differential refractometer. It is apparent that solute and solvent must differ in refractive index, otherwise the solute and its concentration fluctuations are effectively "invisible" in the solvent. The intrinsic difference in the $\tilde{n}$ values of the constituents as well as the concentration of the solution, therefore, determine the small differences in refractive index that must be accurately measured. What is sought is an optical measurement that compares the light interacting with both the solvent and the solution to produce an effect which is sensitive to the refractive index difference. One instrument design for a differential refractometer passes light through a divided cell, the two halves of which contain solvent and solution, respectively. The amount by which the light beam deviates in passing through such a cell is measured by a position-sensitive photodetector. Alternatively, another design uses a split beam to reflect light off the surface of another divided cell, so that part of the beam is reflected by the solvent and part by the solution. The two reflected beams are compared by a dual-element photodetector, and the difference in intensity is related to the difference in $\tilde{n}$. By amplification of the small signals involved, each of these methods is capable of measuring down to 10^{-7} refractive index units under optimum conditions. The usefulness of $d\tilde{n}/dc_2$ as the basis for a detection system in liquid chromatography has contributed to the development of instrumentation in this area.

As noted at the beginning of this section, extrapolation of R_θ to $\theta = 0°$ is one way to correct light-scattering data for interference effects. Interference becomes troublesome for particles whose dimensions are larger than about $\lambda/20$, because light scattered from one portion of the molecule interferes with that scattered by another portion. This situation is shown schematically in Fig. 10.10, which shows the incident light in phase as it passes the surface AA′, but shows different phase relationships in the scattered light at the (distant) surface BB′. It is typical of interference phenomena (think of the colors displayed by a soap film) to show different intensities depending on the angle of observation. Thus in Fig. 10.10 the light scattered at the smaller value of θ remains more nearly in phase than that scattered at the larger angle, where significant destructive interference occurs. This situation is generally true and constitutes the basis for extrapolating to $\theta = 0°$ to eliminate interference effects. The data in Fig. 10.8b were "corrected" in this way.

In the last sentence the word *corrected* is in quotation marks to emphasize the point that the observation *is* corrct: Rather, we are not in a position to deal with the information it tells us, namely, that these particles do not have negligible dimensions compared to λ. Until now we have lacked theory for dealing with this fact. It should be recognized that, by circumventing the

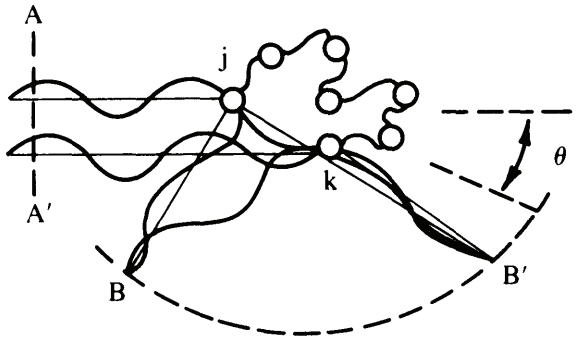

Figure 10.10 Interference of light rays scattered by segments j and k in a polymer chain. Destructive interference increases with increasing θ.

interference effect by extrapolation, we are wasting potentially usable information. Interference occurs in Fig. 10.10 because the light scattered at site j and that scattered at k travel different distances between AA′ and BB′. The wavelength of the light is the "yardstick" that measures this difference in distance traveled. Of course, the latter difference is somehow related to the dimensions of the scattering molecule taken as a whole. Therefore, to bypass this effect by extrapolation is to ignore light as a probe of molecular dimensions. In the next section we shall examine the theory of interference per se, and in Sec. 10.10 we apply the resulting theory to the interpretation of light-scattering data.

10.9 Optical Interference

The Rayleigh scattering theory which culminates in Eq. (10.60) as its most pertinent form for our purposes is based on the explicit assumption that interference effects are absent. The objective of the present section is to correct the Rayleigh theory to allow for interference effects. There are several assumptions-limitations that are implied by our approach:

1. We assume that the Rayleigh theory can be corrected by subdividing the actual solute particle into an array of scattering sites which, considered individually, obey the Rayleigh theory. It can be shown that this approach is a valid approximation so long as $(4\pi R/\lambda)(\tilde{n}_2/\tilde{n}_1 - 1) \ll 1$, where R is the radius of the overall molecule and $\tilde{n}_2$ and $\tilde{n}_1$ are the refractive indices of the solute and solvent, respectively. This shows that the validity of the model involves a trade-off: To apply to progressively larger molecules, the difference in refractive index between solute and solvent must decrease. This particular limitation is not especially severe in polymer applications

of light scattering, but can be a real problem in applications to still larger colloidal particles.

2. We assume that the observed interference is the cumulative effect of the contributions of the individual polymer molecules and that solute-solute interactions do not enter the picture. This effectively limits the model to dilute solutions. This restriction is not particularly troublesome, since our development of the Rayleigh theory also assumes dilute solutions.
3. We assume that there exists a function which we represent by $P(\theta)$—in recognition of the fact that it is angle dependent—which can be multiplied by the scattered intensity as predicted by the Rayleigh theory to give the correct value for i_s, even in the presence of interference. That is,

$$P(\theta) = \frac{i_{s,\text{actual}}}{i_{s,\text{Rayleigh}}} \tag{10.61}$$

4. Based on considerations we have encountered earlier in this chapter, we can anticipate two limiting cases of this function: $P(\theta)$ approaches unity both in the limit of small particles and in the limit of small angles of observation. Interference is absent in both of these cases.

Equation (10.61) suggests how Eq. (10.60), which is valid in the absence of interference, should be corrected. Using Eq. (10.58) for $R_{\theta,\text{Rayleigh}}$, Eq. (10.60) is corrected for interference by dividing both sides of the equation by $P(\theta)$:

$$\frac{Kc_2\,(1+\cos^2\theta)\,I_0}{i_{s,\text{Rayleigh}}\,P(\theta)\,r^2} = \frac{1}{P(\theta)}\left(\frac{1}{M} + 2Bc_2\right) \tag{10.62}$$

Since $P(\theta)\,i_{s,\text{Rayleigh}}$ gives the *observed* scattering intensity at θ—the value that is actually used in the evaluation of R_θ—Eq. (10.62) can be simply written as

$$\frac{Kc_2}{R_\theta} = \frac{1}{P(\theta)}\left(\frac{1}{M} + 2Bc_2\right) \tag{10.63}$$

Our objective now becomes finding an expression for $P(\theta)$.

The theory for $P(\theta)$ proceeds through three stages:

1. We must describe the light scattered with interference in terms of phase differences that develop as the waves pass through a molecule consisting of multiple scattering sites.
2. We must find a way to describe these phase differences in terms of the distances traveled through the array of scattering sites, since this is how the size of the molecule enters the theory.

3. We must average the effect described in item (2) so that no assumed orientation of the scattering sites remains in the final result.

We shall take up these various steps in the following paragraphs.

Figure 10.10 shows that interference is the result of phase differences which arise as the incident light—initially in phase—is scattered by different sites in the molecule. In principle, any particle can be subdivided into a number of hypothetical sites whose isolated behavior is described by the Rayleigh theory. For polymers it is convenient to use the repeat unit of the polymer as the individual scattering site. Thus a polymer whose degree of polymerization is n consists of n independent scattering sites. We can describe each of these by an index number and describe the electric field scattered by the jth using Eq. (10.7), including a phase angle δ_j which is characteristic of the jth repeat unit:

$$E_j = E_0 \cos(2\pi\nu t + \delta_j) \tag{10.64}$$

The net field produced by n such sites is given by

$$E_{net} = \sum_{j=1}^{n} E_j = \sum_{j=1}^{n} E_0 \cos(2\pi\nu t + \delta_j) \tag{10.65}$$

A very useful way to simplify Eq. (10.65) involves the complex number e^{iy} in which $i = \sqrt{-1}$; e^{iy} equals cos y + i sin y. Therefore cos y is given by the real part of e^{iy}. Since exponential numbers are easy to manipulate, we can gain useful insight into the nature of the cosine term in Eq. (10.65) by working with this identity. Remembering that only the real part of the expression concerns us, we can write Eq. (10.65) as

$$E_{0,net}\, e^{i(2\pi\nu t + \delta_{net})} = \sum_{j=1}^{n} E_0\, e^{i(2\pi\nu t + \delta_j)} \tag{10.66}$$

Dividing both sides by $e^{i2\pi\nu t}$ gives

$$E_{0,net}\, e^{i\delta_{net}} = \sum_{j=1}^{n} E_0\, e^{i\delta_j} \tag{10.67}$$

It is the net intensity, not the electric field, which concerns us. We previously used the fact that intensity is proportional to E^2 to evaluate i_s. Using complex numbers to represent E requires one slight modification of this procedure. In the present case we must multiply E by its complex conjugate—obtained by replacing $\sqrt{-1}$ by $-\sqrt{-1}$—to evaluate intensity:

$$i_s \propto \left(\sum_{j=1}^{n} E_0 e^{i\delta_j}\right)\left(\sum_{k=1}^{n} E_0 e^{-i\delta_k}\right) \tag{10.68}$$

where we have introduced k as the index simply to distinguish between the two summations. Equation (10.68) can be written

$$i_s \propto E_0^2 \sum_{j=1}^{n}\sum_{k=1}^{n} e^{i(\delta_j-\delta_k)} \tag{10.69}$$

For every term $\delta_j - \delta_k$ in this double summation, there is a term $\delta_k - \delta_j$ which equals $-(\delta_j - \delta_k)$; therefore Eq. (10.69) is equivalent to

$$i_s \propto \frac{1}{2} E_0^2 \sum_{j=1}^{n}\sum_{k=1}^{n} (e^{i(\delta_j-\delta_k)} + e^{-i(\delta_j-\delta_k)}) \tag{10.70}$$

By using this form, we can take advantage of the identity that $\cos y = 1/2(e^{iy} + e^{-iy})$, from which it follows that

$$i_s \propto E_0^2 \sum_{j=1}^{n}\sum_{k=1}^{n} \cos(\delta_j - \delta_k) \tag{10.71}$$

For Rayleigh scattering, $\delta_j - \delta_k = 0$—there are no phase differences—and each of the cosine terms in Eq. (10.71) equals unity. In this case, which corresponds to $i_{s,\,Rayleigh}$, the right-hand side of Eq. (10.71) equals $E_0^2 n^2$, and we can write

$$\frac{i_s}{i_{s,\,Rayleigh}} = P(\theta) = \frac{1}{n^2} \sum_j \sum_k \cos(\delta_j - \delta_k) \tag{10.72}$$

This expression formalizes the anticipated conclusion that it is the *difference* in phase between light scattered by different segments that is responsible for the interference effect we seek to analyze. Equation (10.72) completes the first of the three stages in the development of $P(\theta)$.

In the next stage of the derivation we replace the difference in phase angles by the difference in the distance traveled by the light in reaching the observer via site j compared with site k. We shall develop this connection for the specific geometry of Fig. 10.11, but in the third stage of the derivation an average for all possible geometries is performed. Hence we need not worry about the specific model for which the second stage is obtained.

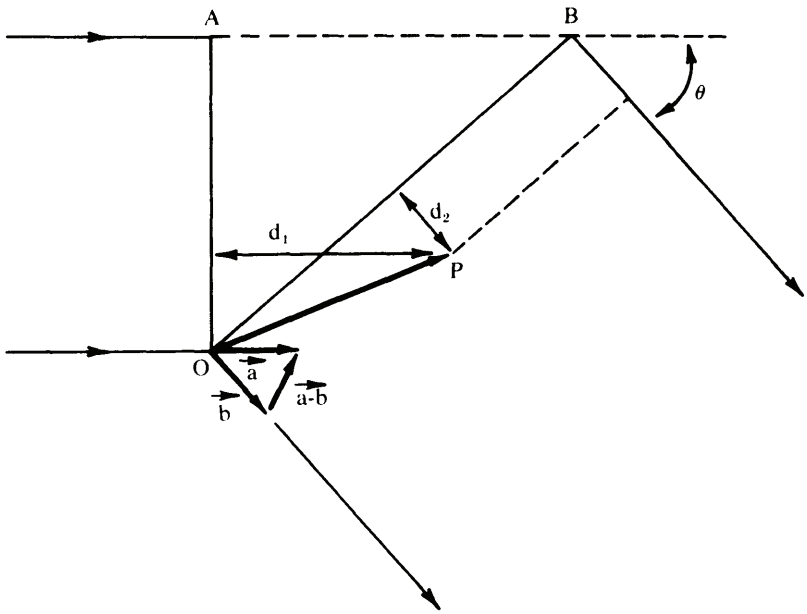

Figure 10.11 Definition of variables required to describe interference of light scattered from points O and P.

Equation (10.72) shows that it is the difference in phase between light scattered by two sites that determines the interference. Hence in Fig. 10.11 we construct two surfaces OA and OB which are perpendicular to the incident and scattered light, respectively. These lines might represent wave crests and, since they meet at O, any segment situated at O is defined to have a phase angle of zero. Suppose we consider a second segment situated at P. To reach a distant observer in the scattering direction, light scattered by a segment located at P must travel a distance d_1 farther in the incident direction compared to a scatterer located at O. In addition, light scattered by a segment at P would have to travel a distance d_2 *less* than light scattered from O to reach the observer. The difference in the distance traveled by light scattered from this pair of sites is therefore given by $d_1 - d_2$. These distances are illustrated in Fig. 10.11. Since there is no phase angle for a scattering segment located at O, the difference in phase angles between O and P can be written

$$\delta_O - \delta_P = \frac{2\pi(d_1 - d_2)}{\lambda} \tag{10.73}$$

Next we look for a relationship between $d_1 - d_2$ and the geometry of the experiment.

The easiest way to proceed is to use vectors to describe this part of the problem. We represent the distance between the pair of scattering sites by the vector $\overrightarrow{OP}$ the length of which is simply r. To express d_1 and d_2 in terms of $\overrightarrow{OP}$ we construct the unit vectors $\vec{a}$ and $\vec{b}$ which are parallel to the incident and scattered directions, respectively. The projection of $\overrightarrow{OP}$ into direction $\vec{a}$, given by the dot product of these two vectors, equals d_1. Likewise, the projection of $\overrightarrow{OP}$ into direction $\vec{b}$ gives d_2. Therefore we can write

$$d_1 - d_2 = \overrightarrow{OP} \cdot \vec{a} - \overrightarrow{OP} \cdot \vec{b} = \overrightarrow{OP} \cdot (\vec{a} - \vec{b}) \tag{10.74}$$

The vector $\vec{a} - \vec{b}$ is also shown in Fig. 10.11 and may be described as the product of a unit vector $\vec{c}$ in the direction $\vec{a} - \vec{b}$ times the scalar length of $\vec{a} - \vec{b}$. This length is easily evaluated, since $\vec{a}$ and $\vec{b}$ are both of unit length and are separated by the angle θ. Therefore a perpendicular to $\vec{a} - \vec{b}$ through O bisects both the angle θ and the length of $\vec{a} - \vec{b}$. The length of $\vec{a} - \vec{b}$ is therefore $2 \sin(\theta/2)$ and we can describe $\vec{a} - \vec{b}$ as

$$\vec{a} - \vec{b} = 2 \sin\left(\frac{\theta}{2}\right) \vec{c} \tag{10.75}$$

Combining Eqs. (10.73)-(10.75) gives

$$\delta_O - \delta_P = \frac{4\pi}{\lambda} \sin\left(\frac{\theta}{2}\right) (\overrightarrow{OP} \cdot \vec{c}) = s(\overrightarrow{OP} \cdot \vec{c}) \tag{10.76}$$

where the scalar quantity s is defined by

$$s = \frac{4\pi}{\lambda} \sin\left(\frac{\theta}{2}\right) \tag{10.77}$$

The phase difference $\delta_O - \delta_P$ given by Eq. (10.76) describes a particular geometrical arrangement between scatterers. This difference can be substituted for the phase difference $\delta_j - \delta_k$ between an arbitrary pair of segments in Eq. (10.72), provided that a suitable averaging is carried out to allow for all possible orientations between segments j and k. We shall take up this averaging in the final stage of the derivation. For now we simply anticipate the average by using an overbar and substitute Eq. (10.76) for $\delta_j - \delta_k$ in Eq. (10.72):

$$P(\theta) = \frac{1}{n^2} \sum_j \sum_k \overline{\cos(s[\overrightarrow{r_{jk}} \cdot \vec{c}])} \tag{10.78}$$

In writing this last result, we have replaced $\overrightarrow{OP}$ by the vector $\overrightarrow{r_{jk}}$ between the generalized pair of segments j and k.

In the final stage of this involved derivation, we have to free Eq. (10.78) from the dependence it contains on the geometry of Fig. 10.11. The problem lies in the dot product of the vector $\overrightarrow{r_{jk}}$—which replaces $\overrightarrow{OP}$ in Fig. 10.11—and $\vec{c}$, the unit vector in the direction $\vec{a} - \vec{b}$ in Fig. 10.11. In Fig. 10.11 these two vectors have a specific orientation with respect to each other, but between an arbitrary pair of segments the vectors are separated by a general angle we call γ. The dot product $\overrightarrow{r_{jk}} \cdot \vec{c}$ then becomes $r_{jk} \cos \gamma$, where r_{jk} is the (scalar) distance between j and k, since the vector $\vec{c}$ has unit length. With this substitution, Eq. (10.78) becomes

$$P(\theta) = \frac{1}{n^2} \sum_j \sum_k \overline{\cos (s r_{jk} \cos \gamma)} \tag{10.79}$$

Now we consider how the averaging implied by the overbar is carried out. What this involves is multiplying $\cos (s r_{jk} \cos \gamma)$ by $P(\gamma)\, d\gamma$—the probability that a particular angle is between γ and $\gamma + d\gamma$—and then integrating the result over all values of γ in keeping with the customary definition of an average quantity.

We can describe the function $P(\gamma)\, d\gamma$ in terms of the same geometrical arrangement shown in Fig. 10.2, with γ replacing ϕ_x. That is, $P(\gamma)\, d\gamma$ is proportional to the area traced on the surface of a sphere by angles in the range γ to $\gamma + d\gamma$:

$$P(\gamma)\, d\gamma = A r \sin \gamma (r\, d\gamma) \tag{10.80}$$

where $A = (\int_0^\pi r^2 \sin \gamma\, d\gamma)^{-1}$ satisfies the normalization criterion. Using this as the expression for $P(\gamma)\, d\gamma$ gives

$$P(\theta) = \frac{1}{n^2} \frac{\int_0^\pi \Sigma_j \Sigma_k \cos (s r_{jk} \cos \gamma) \sin \gamma\, d\gamma}{\int_0^\pi \sin \gamma\, d\gamma} \tag{10.81}$$

This unattractive integral is readily solved by introducing a change of variable in the numerator. If we let $y = s r_{jk} \cos \gamma$, then $dy = -s r_{jk} \sin \gamma\, d\gamma$. The corresponding limits for y—after dividing the range of integration in half and multiplying the integral by 2—are $y = s r_{jk}$ for $\gamma = 0$ and $y = 0$ for $\gamma = \pi/2$. With this change of variable, Eq. (10.81) becomes

$$P(\theta) = \frac{(-2/sr_{jk}) \int_{y=sr_{jk}}^{0} \Sigma_j \Sigma_k \cos y \, dy}{n^2 \, 2 \int_{\gamma=0}^{\pi/2} \sin \gamma \, d\gamma} = \frac{(2/sr_{jk}) \Sigma_j \Sigma_k \sin (sr_{jk})}{2}$$

$$= \sum_j \sum_k \frac{\sin (sr_{jk})}{sr_{jk}} \tag{10.82}$$

This is the result we have sought, although it needs a bit of additional manipulation to make its usefulness evident. The derivation we have followed in this section was developed by Debye in the context of x-ray scattering by the individual atoms of small molecules. Since $s \propto \lambda^{-1}$, this function again emphasizes the idea that R/λ ratios rather than absolute distances themselves are the pertinent quantities in the discussion of optical phenomena. We shall call this theory and its subsequent developments the Debye scattering theory. (Remember that Chap. 2 contains the Debye viscosity theory.) In the next section we examine how Eq. (10.82) can be converted into a practical form.

10.10 The Radius of Gyration

Equation (10.82) is a correct but unwieldy form of the Debye scattering theory. The result benefits considerably from some additional manipulation which converts it into a useful form. Toward this end we assume that the quantity sr_{jk} is not too large, in which case $\sin (sr_{jk})$ can be expanded as a power series. Retaining only the first two terms of the series, we obtain

$$P(\theta) = \frac{1}{n^2} \sum_j \sum_k \frac{\sin (sr_{jk})}{sr_{jk}} = \frac{1}{n^2} \sum_j \sum_k \frac{sr_{jk} - (sr_{jk})^3/3!}{sr_{jk}}$$

$$= \frac{1}{n^2} \sum_j \sum_k \left(1 - \frac{(sr_{jk})^2}{6}\right) \tag{10.83}$$

Since $\Sigma_j \Sigma_k 1 = n^2$, this becomes

$$P(\theta) = 1 - \frac{s^2}{6n^2} \sum_j \sum_k r_{jk}^2 \tag{10.84}$$

At this point it is useful to compare the result we have obtained with the expected behavior of $P(\theta)$ that we anticipated from the definition of this quantity:

1. The smaller the overall dimensions of a molecule, the smaller will be the r_{jk} value for any pair of sites in the molecule. As the values of r_{jk} approach zero, $P(\theta) \to 1$, as required.
2. Equation (10.77) shows that $s \propto \sin(\theta/2)$; therefore $\sin(\theta/2)$ and s approach zero as $\theta \to 0$. This means that $P(\theta) \to 1$ in this limit also, as required.
3. Since the product sr_{jk} appears in Eq. (10.84), there is a trade-off possibility between particle size and the angle of observation. That is, the Debye scattering theory applies with the same level of accuracy to larger molecules at smaller angles and to smaller molecules at larger angles.

Since Eq. (10.63) contains $1/P(\theta)$, since we have already assumed sr_{jk} to be small, and since $1/(1 - y) \cong 1 + y$, Eq. (10.84) can be rewritten as

$$\frac{1}{P(\theta)} = 1 + \frac{s^2}{6n^2} \sum_j \sum_k r_{jk}^2 \tag{10.85}$$

At this point we return to Chap. 1 to connect Eq. (10.85) with the radius of gyration. Although we have not encountered the form $\Sigma_j \Sigma_k r_{jk}^2$ explicitly before, a moment's reflection will convince us that it is identical to the bracketed quantity in Eq. (1.54):

$$\sum_{j=1}^{n} \sum_{k=1}^{n} r_{jk}^2 = \sum_{j=1}^{n} \left(\sum_{k=1}^{j} P(r)\, r^2 + \sum_{k=1}^{n-j} P(r)\, r^2 \right) \tag{10.86}$$

To clarify this identification we note the following:

1. The bracketed summations span the full range of k values from 1 to n and hence can be combined into a single summation.
2. The probability P(r) times r^2 gives a particular value of r^2 which, in the context of Eq. (10.86), is equivalent to r_{jk}^2.
3. Therefore it follows from Eq. (1.54) that

$$\overline{r_g^2} = \frac{1}{2n^2} \sum_j \sum_k r_{jk}^2 \tag{10.87}$$

in the present notation.

Combining Eqs. (10.84) and (10.87) gives

$$\frac{1}{P(\theta)} = 1 + \frac{s^2}{3} \overline{r_g^2} = 1 + \frac{16\pi^2}{3\lambda^2} \overline{r_g^2} \sin^2\left(\frac{\theta}{2}\right) \tag{10.88}$$

Finally, we can incorporate this result into Eq. (10.63) to obtain

$$\left(\frac{Kc_2}{R_\theta}\right)_{c=0} = \frac{1}{M}\left[1 + \frac{16\pi^2}{3\lambda^2}\overline{r_g^2}\sin^2\left(\frac{\theta}{2}\right)\right] \tag{10.89}$$

where the concentration term on the right-hand side of Eq. (10.63) has been omitted, since the Debye scattering theory applies in the limit of $c_2 \to 0$. We see that there is a certain analogy in the way the Rayleigh and the Debye theories must be "corrected":

1. In applying the Rayleigh theory to large polymer molecules, we had to extrapolate results measured at different θ's to $\theta = 0$ to eliminate the interference effect.
2. In applying the Debye theory to concentrated solutions, we must extrapolate the results measured at different concentrations to $c_2 = 0$ to eliminate the effects of solute-solute interactions.
3. Experimentally, R_θ is measured at a series of different c_2's and θ's, which makes the extrapolations of Kc_2/R_θ at constant θ to $c_2 = 0$ and of Kc_2/R_θ at constant c_2 to $\theta = 0$ equally feasible. In the next section we shall examine a specific graphical technique which combines these two extrapolations in a single procedure.

Assuming that concentration effects have been eliminated by extrapolating Kc_2/R_θ to $c_2 = 0$ (subscript $c = 0$), we see that Eq. (10.89) is the equation of a straight line if $(Kc_2/R_\theta)_{c=0}$ is plotted against $\sin^2(\theta/2)$. The characteristic parameters of the line have the following significance:

$$\text{Slope} = \frac{16\pi^2}{3\lambda^2 M}\overline{r_g^2} \tag{10.90}$$

$$\text{Intercept} = \frac{1}{M} \tag{10.91}$$

or

$$\overline{r_g^2} = \frac{3\lambda^2}{16\pi^2}\left(\frac{\text{slope}}{\text{intercept}}\right)_{c=0} \tag{10.92}$$

Figure 10.12 shows data for cellulose nitrate in acetone measured at $\lambda_0 = 436$ nm, and plotted in the manner suggested in Eq. (10.89). The following example completes the analysis of these data.

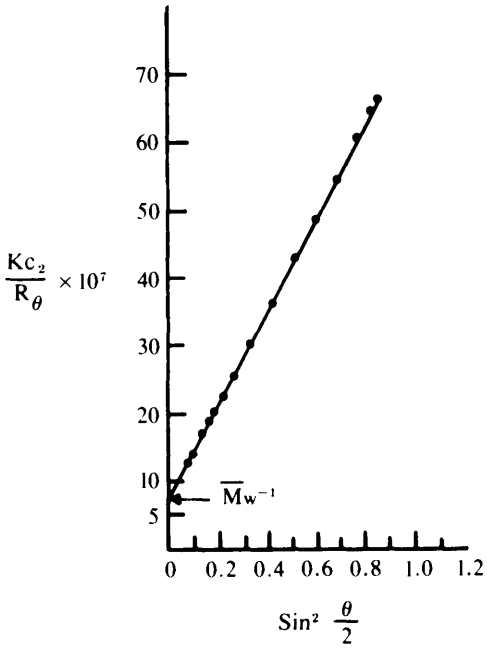

Figure 10.12 Light-scattering data in the limit of $c_2 = 0$ plotted according to Eq. (10.89) for cellulose nitrate in acetone. [Data from H. Benoit, A. M. Holtzer, and P. Doty, *J. Phys. Chem.* 58:635 (1954).]

Example 10.5

Interpret the slope and intercept values of the line in Fig. 10.12 in terms of the molecular weight and radius of gyration of cellulose nitrate in this solution. At 436 nm the refractive index of acetone is 1.359.

Solution

Examination of the graph shows that the line is characterized by the following parameters:

$$\text{Slope} = 6.78 \times 10^{-6} \text{ mol g}^{-1}$$

$$\text{Intercept} = 7.87 \times 10^{-7} \text{ mol g}^{-1}$$

The units of these quantities are determined solely by the ordinate, since the abscissa is dimensionless. Example 10.4 verifies that moles per gram are the units for Kc_2/R_θ. The molecular weight is given by the inverse of the intercept:

$$\bar{M}_w = 1.27 \times 10^6 \text{ g mol}^{-1}$$

Since the intercept corresponds to the Rayleigh limit also (i.e., $\theta = 0°$), Eq. (10.57) demonstrates this to be the weight average value of M.

In acetone $\lambda = \lambda_0/\bar{n} = 436/1.359 = 321$ nm; therefore

$$\overline{r_g^2} = \frac{3\lambda^2 M\,(\text{slope})_{c=0}}{16\pi^2}$$

$$= \frac{3(321 \text{ nm})^2 (1.27 \times 10^6 \text{ g mol}^{-1})(6.78 \times 10^{-6} \text{ mol g}^{-1})}{16\pi^2}$$

$$\overline{r_g^2} = 1.69 \times 10^4 \text{ nm}^2 \qquad \text{or} \qquad (\overline{r_g^2})^{1/2} = r_{g,\text{rms}} = 130 \text{ nm}$$

This distance parameter which characterizes the polymer is about 40% of λ at $\lambda_0 = 436$ nm.

For a polydisperse system not only M but also the radius of gyration will be an average value. Let us next consider the type of average that is obtained for this quantity from light scattering. For this purpose it is sufficient to consider the kind of average obtained for $P(\theta)$: Eq. (10.84) shows that the weighting factor used to average $P(\theta)$ is also that for r_g^2. We proceed as in Sec. 10.7, where we considered the same question for M:

1. We begin with Eq. (10.89)–that is, we neglect solute-solute interactions–and write

$$\frac{Kc_2}{R_\theta} = \frac{1}{\bar{M}_w}\,\frac{1}{\bar{P}(\theta)} \tag{10.93}$$

   This result uses the already established fact that $M = \bar{M}_w$ when the molecular weight is determined by light scattering for a polydisperse system.
2. Equation (10.93) can be written for both the individual components and the mixture as a whole, yielding $Kc_iM_iP_i(\theta) = R_{\theta,i}$ and $Kc_{ex}\bar{M}_w\bar{P}(\theta) = R_{\theta,ex}$, respectively.
3. Since $c_{ex} = \Sigma_i c_i$ and $R_{\theta,ex} = \Sigma_i R_{\theta,i}$, these results can be combined to give

$$\bar{M}_w\,\bar{P}(\theta) = \frac{R_{\theta,ex}}{Kc_{ex}} = \frac{K\Sigma_i M_i c_i P_i(\theta)}{K\Sigma_i c_i} \tag{10.94}$$

4. Because $c_i \propto m_i$, $\bar{M}_w = \Sigma_i c_i M_i / \Sigma_i c_i$; therefore $(\Sigma_i c_i M_i / \Sigma_i c_i)\bar{P}(\theta) = \Sigma_i c_i M_i P_i(\theta)/\Sigma_i c_i$ or

$$\bar{P}(\theta) = \frac{\Sigma_i c_i M_i P_i(\theta)}{\Sigma_i c_i M_i} = \frac{\Sigma_i m_i M_i P_i(\theta)}{\Sigma_i m_i M_i} \tag{10.95}$$

5. Finally, $m_i = n_i M_i$; therefore

$$\bar{P}(\theta) = \frac{\Sigma_i n_i M_i^2 P_i(\theta)}{\Sigma_i n_i M_i^2} \tag{10.96}$$

which shows that the weighting factor for each of the categories averaged is $m_i M_i = n_i M_i^2$. This kind of average is known as a z average. The similarly defined z-average molecular weight, $\bar{M}_z = \Sigma_i n_i M_i^3 / \Sigma_i n_i M_i^2$, is given as Eq. (1.19) in Chap. 1.

Although we presented the derivation for $P(\theta)$ in terms of a random coil, the result is applicable to particles of other geometries–for example, rigid spheres or ellipsoids–provided that the particles fall in the size range where the Debye theory is applicable. The radius of gyration thus obtained is an exact measure of this parameter for the particle in question, regardless of its shape, although its relationship to the physical dimensions of the scatterer does depend on the geometry of the particle. Relationships between the radius of gyration and the dimensions of bodies of various geometries are derived in elementary physics textbooks. Several of these are listed in Table 10.1 for some geometries that are encountered among polymeric solutes. Thus if a particle is known to possess some specific geometry, the radius of gyration can be translated into a geometrical particle dimension through these relationships. It should be emphasized, however, that this type of conversion merely helps us picture the molecule; r_g itself is an equally valid way to describe its dimensions.

In Example 10.5 we extracted both the molecular weight and the radius of gyration from light-scattering data. There may be circumstances, however, when nothing more than the dimensions of the molecule are sought. In this case a simple alternative to the analysis discussed above can be followed. This technique is called the dissymmetry method and involves measuring the ratio of intensities scattered at 45° and 135°. The ratio of these intensities is called the dissymmetry ratio z:

$$z = \frac{i_{s,45°}}{i_{s,135°}} \tag{10.97}$$

This parameter should also be extrapolated to $c_2 = 0$, so the amount of experimental data required in this approach is not significantly less than in the method

Table 10.1 Relationships Between the Radius of Gyration and Geometrical Dimensions for Some Bodies Having Shapes Pertinent to Polymers

Geometry	Definition of parameters	Radius of gyration through the center of gravity
Random coil	$\overline{r^2}$: mean-square end-to-end distance ($\propto n$)	$r_g^2 = \frac{\overline{r^2}}{6}$
Sphere	R: radius of sphere	$r_g^2 = \frac{2}{5} R^2$
Thin rod	L: length of rod (approximation for prolate ellipsoids for which $a/b \gg 1$)	$r_g^2 = \frac{L^2}{12}$
Cylindrical disk	R: radius of disk (approximation for oblate ellipsoids for which $a/b \ll 1$)	$r_g^2 = \frac{1}{2} R^2$

described above. The advantage of working with this quantity, however, is that it can yield a particle dimension with very little calculation through the use of published tables and graphs. To see how this is possible, consider the following points:

1. The factor $1 + \cos^2 \theta$ in R_θ has the same value at $\theta = 45°$ and 135°; hence the ratio $i_{s,45°}/i_{s,135°}$ is the same as $R_{45°}/R_{135°}$ [Eq. (10.58)].
2. Equation (10.63) shows that in the limit of $c_2 = 0$ this ratio also equals the ratio $P(45°)/P(135°)$.
3. By Eq. (10.88), this becomes

$$z = \frac{P(45°)}{P(135°)} = \frac{1 + (16\pi^2/3)(r_g/\lambda)^2 \sin^2 67.5}{1 + (16\pi^2/3)(r_g/\lambda)^2 \sin^2 22.5} \tag{10.98}$$

   and a master curve can be drawn which shows z for different ratios r_g/λ. Of course, this result is subject to the limitations of Eq. (10.88). Especially pertinent is the idea that the particles should not be too large if Eq. (10.98) is used, since large angles are involved.
4. Taking the concept of a master curve a step further, the relationships in Table 10.1 can also be incorporated into such curves so that graphs of z versus a characteristic dimension relative to λ are plotted for various geometries.

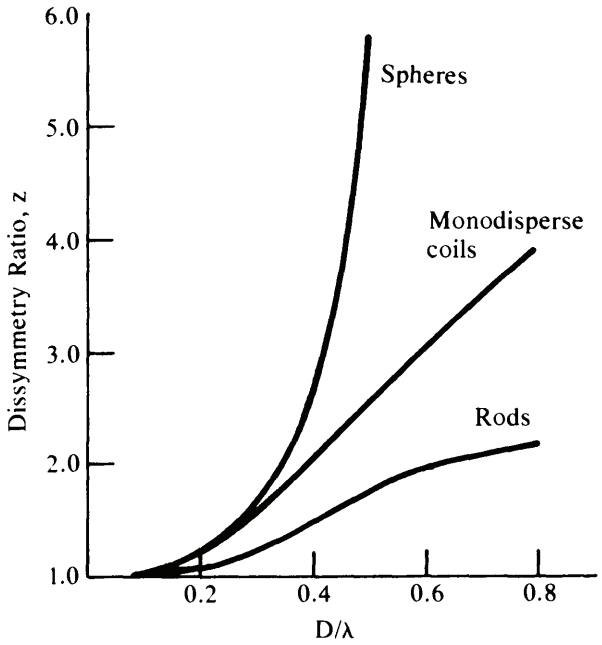

Figure 10.13 Variation of the dissymmetry ratio z with a characteristic dimension D (relative to λ) for spheres, random coils, and rods. (Data from Ref. 4.)

Figure 10.13 shows such plots of z versus D/λ, where D is r_{rms} for random coils, R for spheres and disks, and L for rods. More detailed theories permit these curves to be extended to larger values of r_g/λ than is justified by consideration of Eq. (10.97) alone. In the following example we illustrate an application of this simple method for estimating particle dimensions.

Example 10.6

Poly(γ-benzyl-L-glutamate) is known to possess a helical structure in certain solvents. As part of an investigation† of this molecule, a fractionated sample was examined in chloroform ($CHCl_3$) and chloroform saturated (~0.5%) with dimethyl formamide (DMF). The following results were obtained:

† P. Doty, J. H. Bradbury, and A. M. Holtzer, *J. Am. Chem. Soc.* 78:947 (1956).

	$CHCl_3$	$CHCl_3$ + DMF
$\bar{M}_w$ (g mol^{-1})	144,000	73,000
$(z)_{c=0}$ at 436 nm	1.30	1.11

Taking $\tilde{n} = 1.446$ as the refractive index in both media, estimate the length of the helix in these two situations. Propose a possible interpretation of the results.

Solution

The helix can be approximated as a rod; therefore values of L/λ which are consistent with the observed dissymmetries can be read from Fig. 10.13 or equivalent sources. Also, $\lambda = \lambda_0/\tilde{n} = 436/1.446 = 302$ nm in each of these systems. In view of these considerations, the following results are obtained:

	$CHCl_3$	$CHCl_3$ + DMF
L/λ	0.31	0.19
L (nm)	94	57

The observed molecular weight suggests that this polymer associates into a "dimer" in $CHCl_3$, but that this aggregation is effectively blocked by small amounts of DMF. The particle lengths are not quite in the 2:1 ratio indicative of end-to-end association, but the increase in length is sufficiently large to make such a mechanism worthy of additional study.

•

Until now we have looked at various aspects of light scattering under several limiting conditions, specifically, $c_2 = 0$, $\theta = 0$, or both. Actual measurements, however, are made at finite values of both c_2 and θ. In the next section we shall consider a method of treating experimental data that consolidates all of the various extrapolations into one graphical procedure.

10.11 Zimm Plots

If we substitute Eq. (10.88) into Eq. (10.63) we obtain

$$\frac{Kc_2}{R_\theta} = \left(\frac{1}{M} + 2Bc_2\right)\left[1 + \frac{16\pi^2\overline{r_g^2}}{3\lambda^2}\sin^2\left(\frac{\theta}{2}\right)\right] \tag{10.99}$$

and, since R_θ is measured as a function of both c_2 and θ, this relationship brings together all of the experimental variables and molecular parameters that are

related through light scattering. In the development of this chapter we have looked at special cases of this general function:

1. In the limit of $c_2 = 0$ *and* $\theta = 0^\circ$, $(Kc_2/R_\theta)_{\theta=c=0} = 1/\bar{M}_w$.
2. In the limit of $\theta = 0^\circ$, $(Kc_2/R_\theta)_{\theta=0} = 1/\bar{M}_w + 2Bc_2$.
3. In the limit of $c_2 = 0$, $(Kc_2/R_\theta)_{c=0} = (1/\bar{M}_w)\,[1 + (16\pi^2/3)\,(r_g/\lambda)^2 \sin^2(\theta/2)]$.

The assumptions made in deriving the two factors in Eq. (10.99) restrict the validity of the respective parts of the general expression to these limiting cases. A method for extrapolating experimental data to the limits itemized above has been devloped by Zimm, and the resulting graph—called a Zimm plot—has become a standard way of representing light-scattering data.

There is really nothing in this method that we have not already considered, one aspect at a time, in this chapter. The Zimm plot simply brings it all together in a single analysis.

We shall presently construct a Zimm plot in detail in an example. In anticipation of this, we label each of the paragraphs describing Zimm's procedure for ease of cross-referencing in the example.

1. The method consists of plotting Kc_2/R_θ as the ordinate and $\sin^2(\theta/2) + kc_2$ as the abscissa, where k is a number which is chosen to give a good distribution of data points in the graph. We assign to this constant reciprocal concentration units so that kc_2 can be added to the dimensionless $\sin^2(\theta/2)$. When a suitable scale has been selected, the experimental points are spread over a large area in the graph.
2. Next the points at constant values of c_2 are connected. Likewise, points at constant values of θ are also connected. This produces a grid of intersecting lines that may be straight but which are not necessarily so.
3. On each of the lines that has been drawn, a mark is made at the value of the abscissa corresponding to one of the limiting cases above. Specifically, along the line where $c_2 = c^*$, a mark is placed where the abscissa has the value kc^*. Since the abscissa is $\sin^2(\theta/2) + kc_2$, this mark corresponds to $\theta = 0^\circ$ for this concentration. Similarly, along a line for which $\theta = \theta^*$, a mark is placed where the abscissa equals $\sin^2(\theta^*/2)$. This corresponds to the $c_2 = 0$ limit at this angle.
4. When each of the constant c_2 and constant θ lines has been marked off in this way, the various derived points can be connected. One of these groups of points gives values of Kc_2/R_θ for a range of c's at $\theta = 0^\circ$. The other group of points gives Kc_2/R_θ for a range of θ's at $c_2 = 0$. The two lines thus derived should meet at a common intercept which equals $1/\bar{M}_w$, and their slopes are given by Eqs. (10.55) and (10.90), respectively.

Table 10.2 Values for Kc_2/R_θ at the Indicated Values of θ and c_2 for Solutions of Polystyrene in Benzene at 546 nm

$c_2 \times 10^3$ ($g\ cm^{-3}$)	θ (deg)							
	30	37.5	45	60	75	90	105	120
2.00	3.18	3.26	3.25	3.45	3.56	3.72	3.78	4.01
1.50	2.73	2.76	2.81	2.94	3.08	3.27	3.40	3.57
1.00	2.29	2.33	2.37	2.53	2.66	2.85	2.96	3.12
0.75	2.10	2.14	2.17	2.32	2.47	2.64	2.79	2.93
0.50	1.92	1.95	1.98	2.16	2.33	2.51	2.66	2.79

Source: Data from D. Margerison and G. C. East, *An Introduction to Polymer Chemistry*, Pergamon, Oxford, 1967.

For a sample of polystyrene in benzene, experimental values of Kc_2/R_θ are entered in the body of Table 10.2. The values are placed at the intersection of rows and columns labeled c_2 and θ, respectively. In the following example these values are used to construct a Zimm plot.

Example 10.7

Prepare a Zimm plot using the data in Table 10.2 and evaluate M, B, and $\overline{r_g^2}$ for this solution of polystyrene in benzene. The effective wavelength in the medium is $\lambda_0/\tilde{n} = 546/1.501 = 364$ nm for this experiment.

Solution

We follow the procedure outlined above, cross-referencing the individual steps with the labels introduced above.

1. The abscissa values for the Zimm plot are given by $\sin^2(\theta/2) + kc_2$. For these data, $k = 100\ cm^3\ g^{-1}$ gives a good array of points. Table 10.3 shows the values of the abscissa in the same format used in Table 10.2.
2. Figure 10.14a shows a plot of these data with the lines drawn between points of constant c_2. Likewise, Fig. 10.14b shows the same data with lines drawn between points of constant θ.
3. When $\theta = 0°$, $\sin^2(\theta/2) = 0$ and the abscissa in Fig. 10.14a is simply kc_2. For the solution with $c_2 = 0.5 \times 10^{-3}\ g\ cm^{-3}$, $kc_2 = 0.05$, and this point is marked by an x on the line through the points at this concentration. The x's on other lines in Fig. 10.14a correspond to the $\theta = 0°$ limit for each concentration. When $c_2 = 0$, the abscissa in Fig. 10.14b becomes $\sin^2(\theta/2)$. For the measurements at $\theta = 30°$, $\sin^2 15 = 0.067$, and this

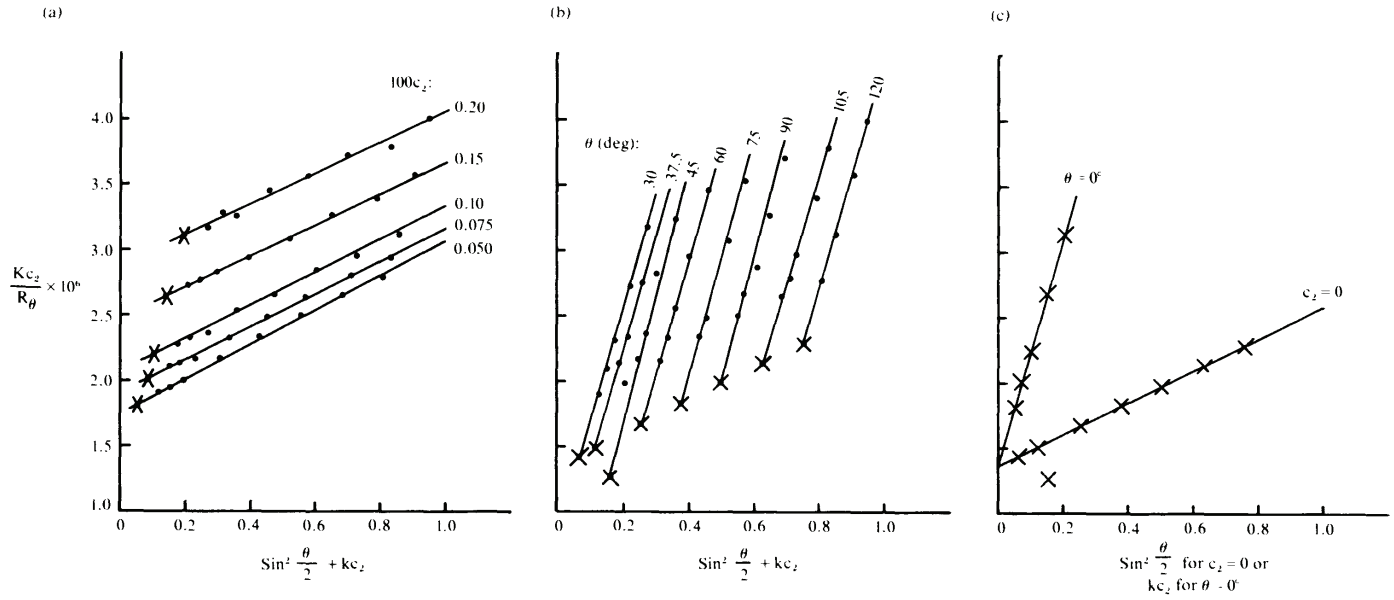

Figure 10.14 Construction of a Zimm plot from the data of Tables 10.2 and 10.3: (a) extrapolation to $\theta = 0°$, (b) extrapolation to $c_2 = 0$, and (c) derived lines.

Table 10.3 Values of $\sin^2(\theta/2) + 100\, c_2$ for the Data in Table 10.2 (used as Abscissa Coordinates in the Construction of Fig. 10.14)

$c_2 \times 10^3$	θ (deg)							
(g cm^{-3})	30	37.5	45	60	75	90	105	120
2.00	0.267	0.303	0.346	0.450	0.571	0.700	0.829	0.950
1.50	0.217	0.253	0.296	0.400	0.521	0.650	0.779	0.900
1.00	0.167	0.203	0.246	0.350	0.471	0.600	0.729	0.850
0.75	0.142	0.178	0.221	0.325	0.446	0.575	0.704	0.825
0.50	0.117	0.153	0.196	0.300	0.421	0.550	0.679	0.800

point is marked by an x on the line through the points at 30°. The x's on the other lines in Fig. 10.14b correspond to the $c_2 = 0$ limit for each angle.

4. Figure 10.14c shows the two limiting lines defined in Figs. 10.14a and b. The derived lines in Fig. 10.14c have the following properties: common intercept = 1.35×10^{-6} mol g^{-1}, slope $c_2 = 0$ line = 1.25×10^{-6} mol g^{-1}, slope $\theta = 0°$ line = 9.0×10^{-6} mol g^{-1} (as drawn), slope $\theta = 0°$ line = 9.0×10^{-4} cm^3 mol g^{-2} (corrected for k). Using Eqs. (10.56) and (10.91), we have

$$\bar{M}_w = \text{intercept}^{-1} = 7.41 \times 10^5 \text{ g mol}^{-1}$$

Using Eq. (10.55), we have

$$B = \frac{(\text{slope})_{\theta=0}}{2} = \frac{9.0 \times 10^{-4}}{2} = 4.5 \times 10^{-4} \text{ cm}^3 \text{ mol g}^{-2}$$

Using Eq. (10.92), we have

$$\overline{r_g^2} = \frac{3\lambda^2}{16\pi^2} \left(\frac{\text{slope}}{\text{intercept}}\right)_{c=0} = \frac{3(364)^2}{16\pi^2} \frac{1.25 \times 10^{-6}}{1.35 \times 10^{-6}} = 2330 \text{ nm}^2$$

$$(\overline{r_g^2})^{1/2} = r_{g,\text{rms}} = 48.2 \text{ nm}$$

•

The objective of the Zimm plot is to conduct all extrapolations on a single graph. The three-stage development of Fig. 10.14 is not typical, but it is intended to clarify the discussion.

Not all Zimm plots show the same grid of essentially parallel straight lines found in Fig. 10.14. In some cases there is considerable curvature, and quite a bit of "interpretation" is required to extract the molecular parameters from the data. In this connection we note that the reciprocal of Eq. (10.83)

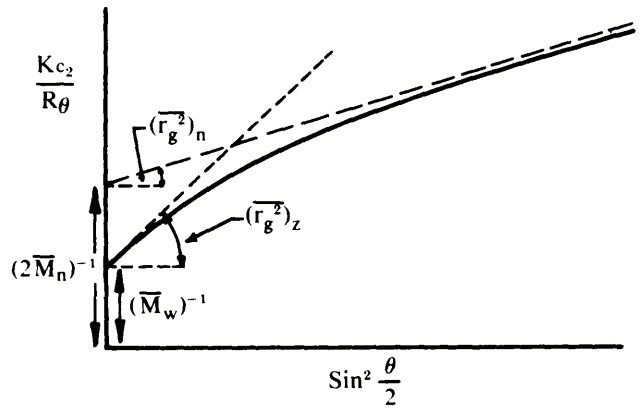

Figure 10.15 Schematic showing alternative limits in the plot of Kc_2/R_θ versus $\sin^2(\theta/2)$ and their interpretation. [Reprinted with permission from H. Benoit, A. M. Holtzer, and P. Doty, *J. Phys. Chem.* 58:635 (1954), copyright 1954 by the American Chemical Society.]

approaches an asymptotic value for large values of sr_{jk}. Instead of Eq. (10.88), the reciprocal of $P(\theta)$ for *large* values of s, r_{jk}, or both (indicated by a prime) is given by

$$\frac{1}{P'(\theta)} = \frac{8\pi^2}{\lambda^2}(\overline{r_g^2})_n \sin^2\left(\frac{\theta}{2}\right) \tag{10.100}$$

In addition, the intercept obtained by extrapolating this asymptote back to $\sin^2(\theta/2) = 0$ equals $(2\overline{M}_n)^{-1}$. Note that both $\overline{M}$ and r_g^2 are *number* averages when this asymptotic limit is used. This is illustrated schematically in Fig. 10.15 and indicates that even more information pertaining to polymer characterization can be extracted from an analysis of the curvature in Zimm plots.

10.12 Appendix: Electrical Units

At one time or another, all of us have tangled with problems of units, but generally these decrease in severity and frequency with experience. Advanced students juggle kilograms and grams, centimeters and angstroms, joules and calories, and rarely fumble in the process. Electrical units are sometimes more troublesome.

In 1785 Coulomb showed that the force between two charges q_1 and q_2 separated by a distance r is proportional to q_1q_2/r^2, a result we know as

Coulomb's law. This relationship poses no particular difficulties as a qualitative statement; the problem arises when we attempt to calculate something with it, since the proportionality constant depends on the choice of units. In the cgs system of units, the electrostatic unit of charge is defined to produce a force of 1 dyne when two such charges are separated by a distance of 1 cm. In the cgs system the proportionality factor in Coulomb's law is unity and is dimensionless. For charges under vacuum we write

$$F_{cgs} = \frac{q_1 q_2}{r^2} \tag{10.101}$$

By contrast, in SI units, the coulomb (C) is the unit of charge and is defined as an ampere second (A sec). To reconcile this with newtons and meters, the units of F and r, respectively, a proportionality constant that is numerically different from unity and which has definite units is required. For charges under vacuum we write

$$F_{SI} = \frac{1}{4\pi\epsilon_0} \frac{q_1 q_2}{r^2} \tag{10.102}$$

where ϵ_0, the permittivity of vacuum, is 8.854×10^{-12} C^2 N^{-1} m^{-2} (or C^2 J^{-1} m^{-1} or kg^{-1} m^{-3} sec^2) and $1/4\pi\epsilon_0$ is 8.988×10^9 N m^2 C^{-2}.

In a medium where the relative dielectric constant is ϵ_r, the force between fixed chages at a definite separation is decreased by the dimensionless factor ϵ_r. This is true regardless of the system of units and is incorporated into Eqs. (10.101) and (10.102) by dividing the right-hand side of each by ϵ_r.

So far, so good. The situation is really no different, say, than the ideal gas law, in which the gas constant is numerically different and has different units depending on the units chosen for p and V. The unit change in Example 10.1 is analogous to changing the gas constant from liter-atmospheres to calories; it is apparent that one system is physically more meaningful than another in specific problems. Several considerations interfere with this straightforward parallel, however, and cause confusion:

1. The fact that the proportionality factor in Eq. (10.101) is numerically equal to unity and is dimensionless makes us tend to forget that any such factor is needed.
2. The fact that the proportionality constant in Eq. (10.102) is not written as, say, k but also includes the factor $(4\pi)^{-1}$ is a recognition of the fact that 4π arises frequently in equations from geometrical considerations and can be conveniently eliminated by this device.

3. In media other than vacuum, the product $\epsilon_0\epsilon_r$ is sometimes written ϵ (no subscript), where ϵ is the permittivity of the medium. Thus in a specific substance, $F_{cgs} \propto 1/\epsilon_r$ and $F_{SI} \propto 1/4\pi\epsilon_r\epsilon_0 = 1/4\pi\epsilon$.
4. In calculation, however, ϵ_r and ϵ are quite different. We must remember that ϵ_r is dimensionless, while ϵ is the product of ϵ_r and ϵ_0, with the latter having definite units.
5. Since the factor 4π is introduced into Eq. (10.102) to encourage cancellation, we frequently find expressions for the same quantity differing by this factor, depending on the system of units used by the author. For example, the Clausius-Mosotti equation [Eq. (10.17)] is written $(4\pi/3)(\rho N_A\alpha/M) = (\epsilon_r - 1)/(\epsilon_r + 2)$ in the cgs system.

Since an electric field E in space is defined as the force experienced by a unit test charge q_t (strictly, in the limit of $q_t \to 0$), it follows that the field produced by q_1 is obtained by letting $q_2 = q_t = 1$ in Coulomb's law:

$$E_{cgs} = \frac{q_1}{\epsilon_r r^2} \tag{10.103}$$

and

$$E_{SI} = \frac{q_1}{4\pi\epsilon_0\epsilon_r r^2} = \frac{q_1}{4\pi\epsilon r^2} \tag{10.104}$$

Even when we discuss the electric field of light without reference to any particular charge, we must be aware of these differences. When that field interacts with a charge, as in light scattering, we will be in trouble unless a self-consistent set of units has been employed.

Problems

1. The geometry of Fig. 10.3 leads to a result known as Snell's law, which relates the refractive index of the medium to the angles formed by two wave fronts with the interface. Defining θ_0 and θ, respectively, as the angles between the phase boundary and the wave front under vacuum and in the medium of refractive index $\tilde{n}$, show that Snell's law requires $\tilde{n} = \sin\theta_0/\sin\theta$.
2. Use the expression given in Example 10.3 to evaluate the compressibility of CCl_4 from the fact† that $R_{90} = 5.38 \times 10^{-4}$ m^{-1} at room temperature for $\lambda_0 = 546$ nm. The depolarization ratio $\rho_u(90)$ is 0.042 for this liquid and $\tilde{n} = 1.460$, $\alpha = 1.21 \times 10^{-3}$ deg^{-1}, and $d\tilde{n}/dT = 58.6 \times 10^{-5}$ deg^{-1}. Compare the light-scattering value with a literature value for β_{CCl_4}; be sure to cite the reference consulted.

† Data from Ref. 3.

3. Fowle† measured the turbidity of air at Mt. Wilson, California, on a clear day in 1913. Values of τx for dry air at different wavelengths are tabulated below, where x is essentially the thickness of the atmosphere corrected to standard temperature and pressure (STP) conditions:

λ (μm)	τx	λ (μm)	τx
0.3504	0.459	0.5026	0.122
0.3600	0.423	0.5348	0.108
0.3709	0.377	0.5742	0.100
0.3838	0.338	0.5980	0.091
0.3974	0.285	0.6238	0.074
0.4127	0.245	0.6530	0.064
0.4307	0.213	0.6858	0.0419
0.4516	0.174	0.7222	0.0304
0.4753	0.147	0.7644	0.0212

Prepare a log-log plot of τx versus λ and evaluate the slope as a test of the Rayleigh theory applied to air. The factor $M/\rho N_A$ in Eq. (10.36) becomes $6.55 \times 10^5/N_0$, where N_0 is the number of gas molecules per cubic centimeter at STP and the numerical factor is the thickness of the atmosphere corrected to STP conditions. Use a selection of the above data to determine several estimates of N_0, and from the average, calculate Avogadro's number. The average value of $\tilde{n} - 1$ is 2.97×10^{-4} over the range of wavelengths which are most useful for the evaluation of N_A.

4. Bhatnagar and Biswas‡ measured the turbidity at 436 nm of a *single* sample of poly(methyl methacrylate) in several solvents, including acetone and methyl ethyl ketone (MEK):

	$d\tilde{n}/dc_2$	$(Hc_2/\tau)_{c=0}$	M
In acetone	0.13914	1.75×10^{-6}	571,000
In MEK	0.01385	2.60×10^{-8}	38,400,000

Working with different samples of the same polymer, other researchers have published conflicting values for the refractive index gradient in these solvents:

	$d\tilde{n}/dc_2$ in acetone	$d\tilde{n}/dc_2$ in MEK
Cohn and Schuele §	0.137	0.113
Tremblay et al.#	0.107	0.093

† F. E. Fowle, *Astrophys. J.* 40:435 (1914).
‡ H. L. Bhatnagar and A. B. Biswas, *J. Polym. Sci.* 13:461 (1954).
§ E. S. Cohn and E. M. Schuele, *J. Polym. Sci.* 14:309 (1954).
# R. Tremblay, Y. Sicotte, and M. Rinfret, *J. Polym. Sci.* 14:310 (1954).

Using the original Hc_2/τ values, recalculate M using the various refractive index gradients. On the basis of self-consistency, estimate the molecular weight of this polymer and select the best value of $d\bar{n}/dc_2$ in each solvent. Criticize or defend the following proposition: Since the extension of the Debye theory to large particles requires that the difference between $\bar{n}$ for solute and solvent be small, this difference should routinely be minimized for best results.

5. Various amounts of either ethanol or hexane were added to polystyrene solutions in benzene and τ was measured for several concentrations of polymer. The following results were obtained† (c_2 in g liter^{-1}; Hc_2/τ in mol g^{-1}):

Pure benezene	
c_2	$Hc_2/\tau \times 10^6$
0.73	1.47
1.21	1.82
2.00	2.38

Benzene + percent ethanol			
20%		28.5%	
c_2	$Hc_2/\tau \times 10^6$	c_2	$Hc_2/\tau \times 10^6$
0.52	0.75	0.52	0.51
1.06	0.87	1.00	0.56
1.60	1.00	–	–

Benzene + percent hexane			
50%		58%	
c_2	$Hc_2/\tau \times 10^6$	c_2	$Hc_2/\tau \times 10^6$
0.28	0.95	0.28	0.89
0.66	1.00	0.66	0.89
0.88	1.06	0.88	0.91

Evaluate M and B for each of the five runs on this polymer sample and comment on the following points:

a. What is the significance of the runs for which $B \cong 0$?
b. What is the significance of the difference in the amount of the two diluents needed to produce the $B = 0$ condition?
c. What is the significance of the different behavior with respect to M for the two diluents?

† E. D. Kunst, *Rec. Trav. Chim. Pays Bas* 69:125 (1950).

6. Zimm† has reported the intensity of scattered light at various angles of observation for polystyrene in toluene at a concentration of 2×10^{-4} g cm^{-3}. The following results were obtained (values marked * were estimated and not measured):

θ (deg)	i_s (arbitrary units)
0	4.29*
25.8	3.49
36.9	2.89
53.0	2.18
66.4	1.74
90.0	1.22
113.6	0.952
143.1	0.763
180	0.70*

Draw a plot in polar coordinates of the scattering envelope in the xy plane. How would the envelope of a Rayleigh scatterer compare with this plot? By interpolation, evaluate i_{45}, i_{135}, and z. Use Fig. 10.13 to estimate the value of r_{rms} to which this dissymmetry ratio corresponds if λ (in toluene) is 364 nm. What are some practical and theoretical objections to this procedure for estimating r_{rms}?

7. The effect of adenosine triphosphate (ATP) on the muscle protein myosin was studied by light scattering in an attempt to resolve conflicting interpretations of viscosity and ultracentrifuge data. The controversy hinged on whether the myosin dissociated or changed molecular shape by interaction with ATP. Blum and Morales‡ reported the following values of $(Kc_2/R_\theta)_{c=0}$ versus $\sin^2(\theta/2)$ for myosin in 0.6 M KCl at pH 7.0:

$\sin^2(\theta/2)$	0.15	0.21	0.29	0.37	0.50	0.85
$Hc_2/\tau \times 10^7$						
(Before ATP)	0.9	1.1	1.5	1.8	2.2	2.7
(During ATP)	1.9	2.8	3.7	4.6	6.0	6.8

Which of the two models for the mode of ATP interaction with myosin do these data support? Explain your answer by quantitative interpretation of the light-scattering data.

† B. H. Zimm, *J. Chem. Phys.* 16:1093 (1948).

‡ J. J. Blum and M. F. Morales, *Arch. Biochem. Biophys.* 43:208 (1953).

8. Aggregation of fibrinogen molecules is involved in the clotting of blood. To learn something about the mechanism of this process, Steiner and Laki† used light scattering to evaluate M and the length of these rod-shaped molecules as a function of time after a change from stable conditions. The stable molecule has a molecular weight of 540,000 g mol^{-1} and a length of 840 Å. The following table shows the average molecular weight and average length at several times for two different conditions of pH and ionic strength μ:

pH = 8.40 and μ = 0.35 M			pH = 6.35 and μ = 0.48 M		
t (sec)	M × 10^{-6} (g mol^{-1})	length (Å)	t (sec)	M × 10^{-6} (g mol^{-1})	length (Å)
650	1.10	1300	900	1.10	1100
1150	1.65	1600	1000	2.0	1200
1670	2.20	1900			
2350	3.30	2200			

Criticize or defend the following proposition: The apparent degree of aggregation x at various times can be obtained in terms of either the molecular weight *or* the length. The ratio of the values of x based on M to that based on length equals unity for exclusively end-to-end aggregation and increases from unity as the proportion of edge-to-edge aggregation increases. In the higher pH-lower μ experiment there is considerably less end-to-end aggregation in the early stages of the process than in the lower pH-higher μ experiment.

9. Zimm plots at 546 nm were prepared for a particular polystyrene at two temperatures and in three solvents. The following summarizes the various slopes and intercepts obtained‡:

	T = 22°C		
Solvent	Intercept	$\left(\frac{\text{slope}}{\text{intercept}}\right)_{c=0}$	$\left(\frac{\text{slope}}{\text{intercept}}\right)_{\theta=0}$
Methyl ethyl ketone	0.896	0.608	260
Dichloroethane	1.61	1.16	900
Toluene	3.22	1.14	1060

† R. F. Steiner and K. Laki, *Arch. Biochem. Biophys.* 34:24 (1951).
‡ P. Outer, C. I. Carr, and B. H. Zimm, *J. Chem. Phys.* 18:830 (1950).

	T = 67°C		
Solvent	Intercept	$\left(\frac{\text{slope}}{\text{intercept}}\right)_{c=0}$	$\left(\frac{\text{slope}}{\text{intercept}}\right)_{\theta=0}$
Methyl ethyl ketone	0.840	0.551	230
Dichlorethane	1.50	1.05	870
Toluene	2.80	1.09	800

The slope–intercept ratios have units of cubic centimeters per gram, and the intercepts are $c/R_{\theta,v}$, where the subscript v indicates vertically polarized light. In this case $K_v = 4\pi^2 (\tilde{n}d\tilde{n}/dc_2)^2/\lambda_0^4 N_A$. The following values of $\tilde{n}$ and $d\tilde{n}/dc_2$ can be used to evaluate K_v:

	T = 20° C ≅ 22°C		T = 67°C	
	$\tilde{n}$	$d\tilde{n}/dc_2$	$\tilde{n}$	$d\tilde{n}/dc_2$
Methyl ethyl ketone	1.378	0.221	1.359	0.230
Dichloroethane	1.444	0.158	1.423	0.167
Toluene	1.496	0.108	1.472	0.118

Evaluate M, $(\overline{r_g^2})^{1/2}$, and B from each piece of pertinent data and comment on the following points:

a. Agreement between M values.
b. Correlation of $(\overline{r_g^2})^{1/2}$ and B with solvent "goodness."

10. For polystyrene in butanone at 67°C the following values of $Kc_2/R_\theta \times 10^6$ were measured† at the indicated concentrations and angles. Construct a Zimm plot from the data below using k = 100 $cm^3\ g^{-1}$ for the graphing constant. Evaluate M, B, and $(\overline{r_g^2})^{1/2}$ from the results. In this experiment λ_0 = 546 nm and $\tilde{n}$ = 1.359 for butanone at this temperature.

	c_2 (g cm^{-3})	
θ (deg)	1.9×10^{-3}	3.8×10^{-4}
25.8	–	1.48
36.9	1.84	1.50
53.0	1.93	1.58
66.4	1.98	1.62
90.0	2.10	1.74
113.6	2.23	1.87
143.1	2.34	1.98

† B. H. Zimm, *J. Chem. Phys.* 16:1093 (1948).

11. Benoit et al.† prepared a mixture of two different fractions of cellulose nitrate and determined the molecular weight of the mixture by light scattering. The mixture was 25.8% by weight fraction A and 74.2% fraction B, where the individual fractions have the following properties:

Fraction	$\bar{M}_n$	$\bar{M}_w$
A	635,000	1,270,000
B	199,000	400,000

Calculate $\bar{M}_n$ and $\bar{M}_w$ for the mixture on the basis of this information concerning the components and their proportions. The following light-scattering data for the mixture allow $\bar{M}_n$ and $\bar{M}_w$ to be evaluated by the procedure shown in Fig. 10.15:

θ (deg)	$(Kc_2/R_\theta) \times 10^7$ (mol g^{-1})	θ (deg)	$(Kc_2/R_\theta) \times 10^7$ (mol g^{-1})
30	19.6	80	42.2
35	21.7	90	48.7
40	24.4	100	53.0
45	26.4	110	57.0
50	28.3	120	61.3
55	31.0	130	64.9
60	33.0	140	67.4
70	37.4		

Evaluate $\bar{M}_n$ and $\bar{M}_w$ from the light-scattering data and compare the values with those calculated from the preparation of the mixture.

Bibliography

1. Dover, S. D., in *An Introduction to the Physical Properties of Large Molecules in Solution*, by E. G. Richards, Cambridge University Press, Cambridge, 1980.
2. Hiemenz, P. C., *Principles of Colloid and Surface Chemistry*, Marcel Dekker, New York, 1977.
3. Kerker, M., *The Scattering of Light and Other Electromagnetic Radiation*, Academic, New York, 1969.
4. Stacey, K. A., *Light Scattering in Physical Chemistry*, Butterworths, London, 1956.
5. Tanford, C., *The Physical Chemistry of Macromolecules*, Wiley, New York, 1961.

† H. Benoit, A. M. Holtzer, and P. Doty, *J. Phys. Chem.* 58:635 (1954).